Georgia Institute of Technology
Atlanta, Georgia 30332

SEMI-ANNUAL REPORT

ANALYSIS OF DELAMINATION RELATED FRACTURE PROCESSES IN COMPOSITES

NASA GRANT NAG-1-637
GEORGIA TECH PROJECT E16-654

PRINCIPAL INVESTIGATOR
Erian A. Armanios

SEMI-ANNUAL REPORT

EFFECT OF DAMAGE ON ELASTICALLY TAILORED COMPOSITES

NASA GRANT NAG-1-637
GEORGIA TECH PROJECT E16-654

PRINCIPAL INVESTIGATOR
Erian A. Armanios

This report covers the research work performed for the period starting September 1991 and ending February 1992. An investigation of the different physical contributions in the displacement field derived from the variationally asymptotical analysis is performed. The analytical approach along with the derived displacement field and stiffness coefficients for a generally anisotropic thin-walled beam is presented in detail in Ref.1. A copy is attached in the Appendix for convenience.

Significance of Out-of-plane Warping

The variationally asymptotical approach does not require an a priori assumed displacement field and the warping function emerges as natural result. It follows an iterative process. The displacement function corresponding to the zeroth order approximation is obtained first by keeping the leading order terms in the energy functional. A set of successive corrections is added and the associated energy functional is determined. Corrections generating terms of the same order in the energy functional as previously obtained, are kept. The process is terminated when the new contributions generate terms of smaller order. The displacement field converges to the following expression:

$$
\begin{aligned}
v_1 &= U_1(x) - y(s)U_2'(x) - z(s)U_3' + G(s)\varphi'(x) \\
&\quad + \underline{g_1(s)U_1'(x) + g_2(s)U_2''(x) + g_3(s)U_3''(x)} \\
v_2 &= U_2(x)\frac{dy}{ds} + U_3(x)\frac{dz}{ds} + \varphi(x)r_n \\
v &= U_2(x)\frac{dz}{ds} - U_3(x)\frac{dy}{ds} - \varphi(x)r_t
\end{aligned}
\tag{1}
$$

The axial displacement is denoted by v_1 while v_2 and v denote the displacement along the tangent and normal to the cross section mid-surface, respectively as shown in Fig.1. The average displacement over the cross section along the x, y and z Cartesian coordinate system is denoted by $U_1(x)$, $U_2(x)$ and $U_3(x)$, respectively. The cross sectional rotation is denoted by $\phi(x)$. The underlined terms in Eq.(1) represent the extension and bending-related warping. These new terms emerges naturally in addition to the classical torsional-related warping $G(s)\ \phi'$. They are strongly

influenced by the material's anisotropy and vanish for materials that are either orthotropic or whose properties are antisymmetric relative to middle surface of the cross section wall. These out-of-plane warping functions were derived earlier and presented in Ref.2.

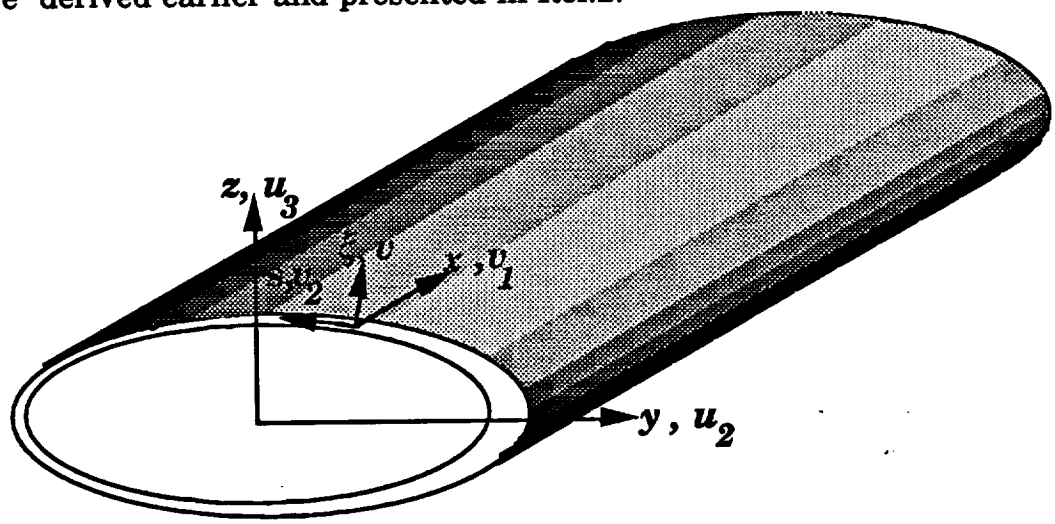

Fig.1 Coordinate system

The contribution of out-of-plane warping was considered recently by Kosmatka [*3*]. Local in-plane deformations and out-of-plane warping of the cross section were expressed in terms of unknown functions. These functions were assumed to be proportional to the axial strain, bending curvature and twist rate within the cross section and were determined using a finite element modeling. In our formulation, the out-of-plane warping is shown to be proportional to the axial strain, bending curvature and twist rate. Moreover, the functions associated with each physical behavior are expressed in closed-form by $g_1(s)$ for the axial strain, $g_2(s)$ and $g_3(s)$ for the bending curvatures and $G(s)$ for the twist rate.
An illustration of their effect appears in Figs. 2 and 3 where the bending slope in a cantilevered beam is plotted along the span. The beam is subjected to a unit bending load at the tip and has a rectangular cross section with $[15]_6$ (Fig.2) and $[30]_6$ (Fig.3) layup. Two types of predictions are compared to the experimental results [*4, 5*]. In the first, the torsional-related warping is considered only while in the second the contribution of bending-related warping is included. Extension-related warping is negligible for this construction. Neglecting bending-related warping leads to significant errors in predictions for this case.

Shear Deformation Contribution

A similar behavior to the one illustrated in Figs. 2 and 3 was found in the theory of Ref. 5 when the shear deformation contribution is neglected. This may indicate that the out-of-plane warping due to bending includes implicitly the shear deformation contribution. In the theory of Ref.5 the cross section stiffness coefficients are predicted from a finite element

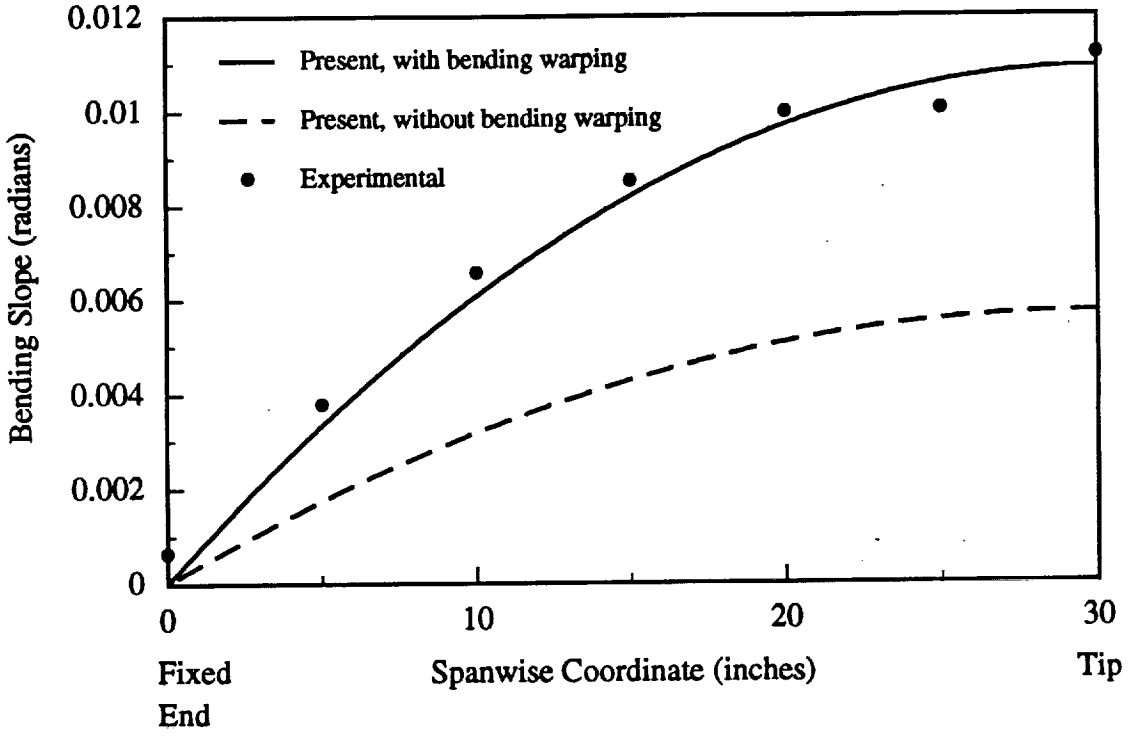

Fig. 2 Bending slope in a $[15]_6$ cantilevered beam under unit tip load

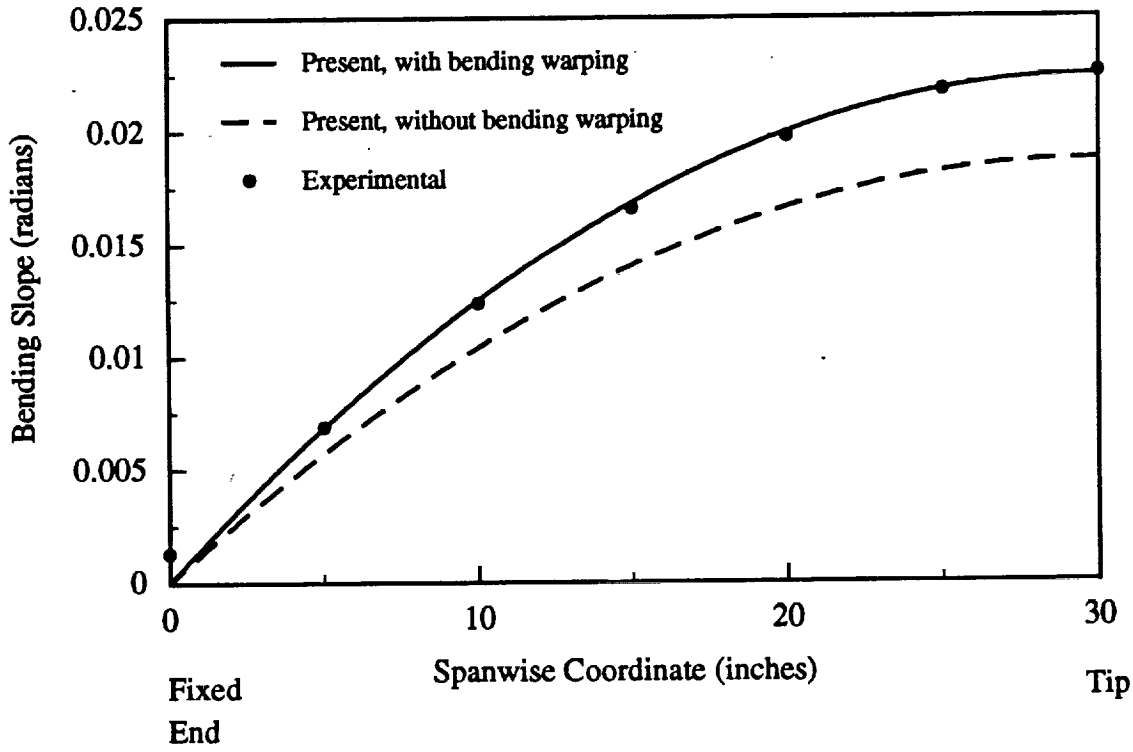

Fig. 3 Bending slope in a $[30]_6$ cantilevered beam under unit tip load

simulation. The theory is not restricted to thin-walled configurations. In order to assess the similarity between the shear deformation contribution and the out-of-plane warping, the present theory and the numerical work of Ref. 5 are applied to the prediction of the deflection curve in a cantilevered beam made of graphite/epoxy material and subjected to a transverse tip load of 1 lb. The beam has a $[15]_6$ layup with a rectangular cross section. The geometry and mechanical properties are similar to those of Ref. 5 and are provided in Table I.

Table I. Cantilever Geometry and Properties

Ply Thickness = 0.005 in
Width = 0.923 in.
Depth = 0.50 in.
E_{11} = 20.6 Msi.
E22 = E33 = 1.42 Msi.
G_{12} =G_{13} = 0.87 Msi.
G_{23} = 0.696 Msi
$\upsilon_{12} = \upsilon_{13} = 0.30$
$\upsilon_{23} = 0.34$

Figure 4 shows a similar behavior suggesting that in the present theory, shear deformation is implicitly accounted through bending-related warping. The prediction of Ref.5 are referred to as Classical when shear deformation is neglected. Further evidence could be provided by estimating the equivalent shear deformation strain in the present theory which can be expressed in terms of the slope of the plane that approximates the cross section warping. This slope is given by

$$2\gamma_{xy} = -\frac{\int y v_1 dA}{I_{zz}} \tag{2}$$

where A and I_{zz} denote the cross-sectional area and second moment of area about the z-axis, respectively. A comparison of the shear strain γ_{xy} over the length of the beam with the prediction of Ref. 5. is shown in Fig. 5.

The shear strain at the fixed end is 4.5924×10^{-4} based on Eq.(2) which is within 2 % of 4.6857×10^{-4} calculated on the basis of Ref. 5.

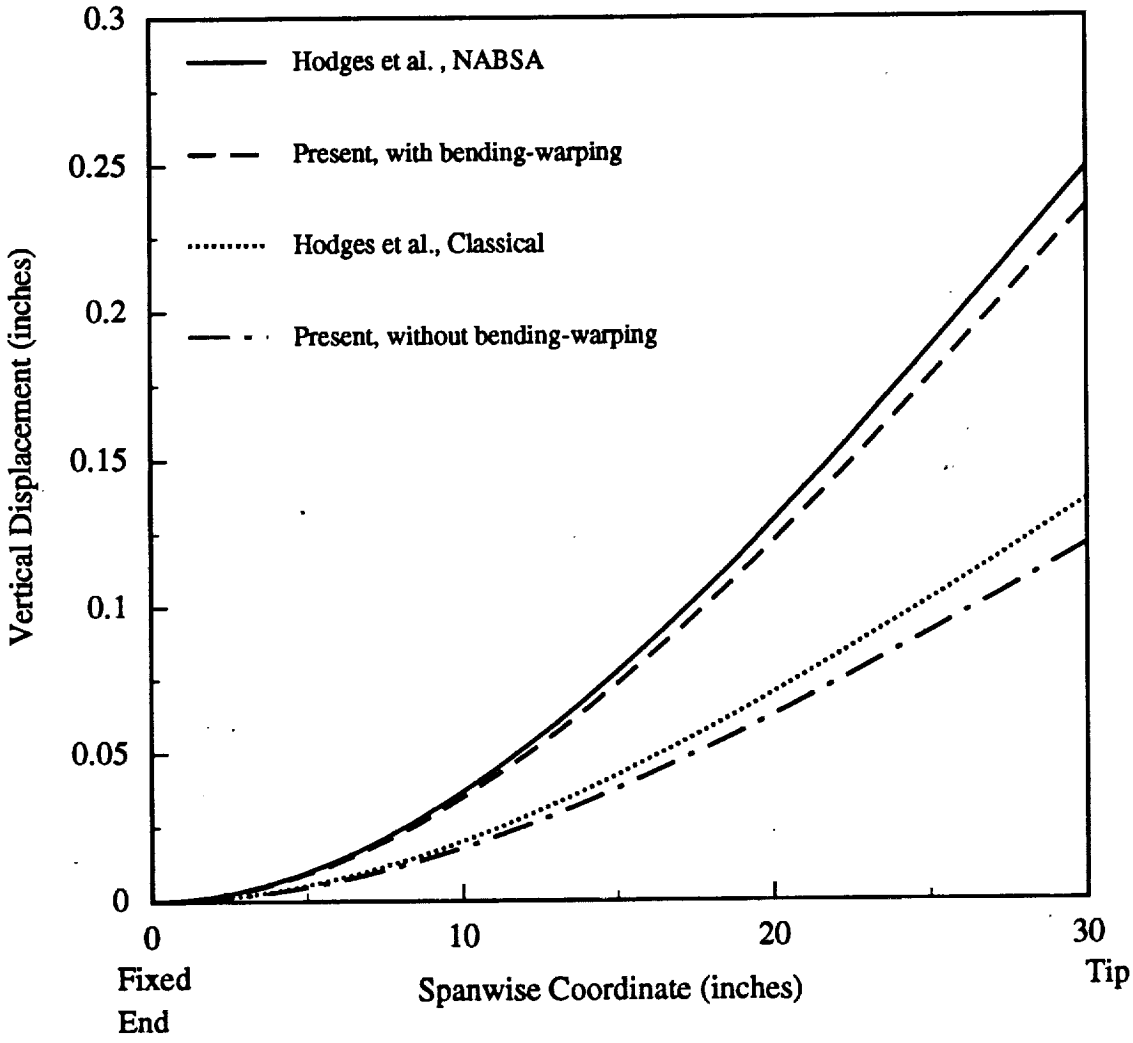

Fig. 4 Deflection of a $[15]_6$ cantilevered beam under unit tip load

Closing Remarks

The variationally asymptotical theory developed provides a consistent means for including the effects of the material's anisotropy in thin-walled beams. Two issues have been addressed in this progress report. The first, is concerned with the functional form of in-plane deformation and out-of-plane warping contributions to the displacement field. The second, is concerned with the significance of shear deformation effects.

A rigorous proof is provided for the assumed displacement field in Kosmatka's work [3]. Local in-plane deformations and out-of-plane warping of the cross section are indeed shown to be proportional to the axial strain, bending curvature and twist rate within the cross section. Moreover, their closed form functions are determined.

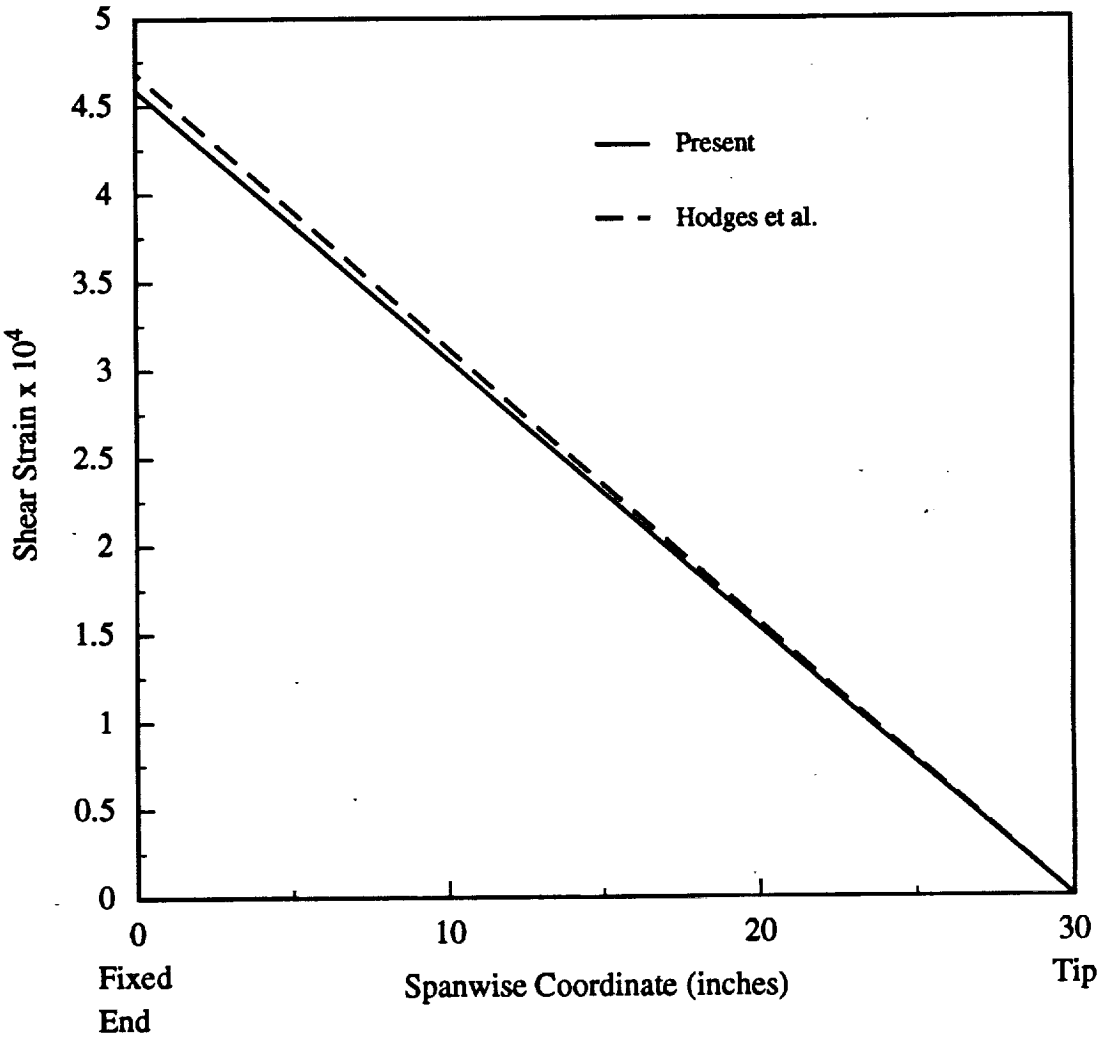

Fig. 5 Shear strain in a $[15]_6$ cantilevered beam under unit tip load

The significance of shear deformation in the modeling of laminated composites was recognized in the early work of Rehfield and was followed by Chopra et al. by adopting a Timoshenko-type shear deformation formulation. The displacement field developed in the present work is shown to include shear deformation through the out-of-plane warping terms. A closed form expression for the slope of the plane that approximates the cross section warping is derived and shown to be within 2% of the shear strain in a cantilever beam problem.

REFERENCES

[1]. Berdichevsky, V., Armanios, E., and Badir, A., "Theory of Anisotropic Thin-Walled Closed Cross-Section Beams", To appear in a special issue of *Composites Engineering*, May 1992.

[2] Armanios, E., Badir, A., and Berdichevsky, V., "Effect of damage on Elastically Tailored Composite Laminates", *Proceedings of the AHS International Technical Specialists' Meeting on Rotorcraft Basic Research,* Georgia Institute of Technology, Atlanta, Georgia, March 25-27, 1991, pp. 48(1)-48(11).

[3]. Kosmatka, J. B., "Extension-bend-Twist Coupling Behavior of Thin-walled Advanced Composite Beams with Initial Twist," *Proceedings of the 32st AIAA/ASME/AHS/ASC Structures, Structural Dynamics and Materials Conference*, 1991, pp. 1037-1049.

[4]. Smith, E. C., and Chopra, I., "Formulation and Evaluation of an Analytical Model for Composite Box-Beams," in Proceedings of the *31st AIAA/ASME/AHS/ASC Structures, Structural Dynamics and Materials Conference*, 1990, pp. 759-782

[5]. Smith, E. C., and Chopra, I., "Formulation and Evaluation of an Analytical Model for Composite Box-Beams," *Journal of the American Helicopter Society*, July 1991, pp. 23-35.

[6]. Hodges, D. H., Atilgan, A. R., Cesnik, C. S., and Fulton, M. V., "On a Simplified Strain Energy Function for Geometrically Nonlinear Behavior of Anisotropic Beams," Presented at the Seventeenth European Rotorcraft Forum, September 24-26, 1991, Berlin, Germany. To appear in a special issue of *Composites Engineering*, May 1992

APPENDIX

Paper to appear in a special issue of *Composites Engineering*, May 1992

Theory of Anisotropic Thin-Walled Closed Cross-Section Beams

Victor Berdichevsky, Erian Armanios, and Ashraf Badir *
School of Aerospace Engineering
Georgia Institute of Technology
Atlanta, Georgia 30332-0150

ABSTRACT

A variationally and asymptotically consistent theory is developed in order to derive the governing equations of anisotropic thin-walled beams with closed sections. The theory is based on an asymptotical analysis of two-dimensional shell theory. Closed-form expressions for the beam stiffness coefficients, stress and displacement fields are provided. The influence of material anisotropy on the displacement field is identified. A comparison of the displacement fields obtained by other analytical developments is performed. The stiffness coefficients and static response are also compared with finite element predictions, closed form solutions and test data.

INTRODUCTION

Elastically tailored composite designs are being used to achieve favorable deformation behavior under a given loading environment. Coupling between deformation modes such as extension-twist or bending-twist is created by an appropriate selection of fiber orientation, stacking sequence and materials. The fundamental mechanism producing elastic tailoring in composite beams is a result of their anisotropy. Several theories have been developed for the analysis of thin-walled anisotropic beams.

*Professor, Associate Professor, and Graduate Research Assistant, respectively.

A review is provided in Hodges (1990). A basic element in the analytical modeling development is the derivation of the effective stiffness coefficients and governing equations which allows the three-dimensional ($3D$) state of stress to be recovered from a one-dimensional ($1D$) beam formulation. For isotropic or orthotropic materials this is a classical problem, which is considered in a number of text books such as Timoshenko and Goodier (1951), Sokolnikoff (1956), Washizu (1968), Crandall *et al.* (1978), Wempner (1981), Gjelsvik (1981), Libai and Simmonds (1988), and Megson (1990).

For generally anisotropic materials a number of $1D$ theories have been developed by Reissner and Tsai (1972), Mansfield and Sobey (1979), Rehfield (1985), Libove (1988), Rehfield and Atilgan (1989), and Smith and Chopra (1990;1991). A discussion of these works is provided in the comparison section of this paper.

The objective of this work is to develop a consistent theory for thin-walled beams made of anisotropic materials. The theory is an asymptotically correct first order approximation. The accuracy of previously developed theories is assessed by comparing the resulting displacement fields. A comparison of stiffness coefficients and static response with finite element predictions, closed form solutions and test data is also performed.

A detailed derivation of the theory is presented first. This is followed by a summary of governing equations. Finally a comparison of results with previously developed theories is provided.

DEVELOPMENT OF THE ANALYTICAL MODEL

Coordinate Systems

Consider the slender thin-walled elastic cylindrical shell shown in Fig. 1. The length of the shell is denoted by L, its thickness by h, the radius of curvature of the middle surface by R and the maximum cross sectional dimension by d. It is assumed that

$$d << L \qquad h << d \qquad h << R \tag{1}$$

The shell is loaded by external forces applied to the lateral surfaces and at the ends. It is assumed that the variation of the external forces and material properties over distances of order d in the axial direction and over distances of order h in the

circumferential direction, is small. The material is anisotropic and its properties can vary in the direction normal to the middle surface.

It is convenient to consider simultaneously two coordinate systems for the description of the state of stress in thin-walled beams. The first one is the Cartesian system x, y and z shown in Fig. 1. The axial coordinate is x while y and z are associated with the beam cross section. The second coordinate system, is the curvilinear system x, s and ξ shown in Fig. 2. The circumferential coordinate s is measured along the tangent to the middle surface in a counter-clockwise direction whereas ξ is measured along the normal to the middle surface. A number of relationships have a simpler form when expressed in terms of curvilinear coordinates. A relationship between the two coordinate systems can be established as follows.

Define the position vector $\vec{r}$ of the shell middle surface as

$$\vec{r} = x\vec{i}_x + y(s)\vec{i}_y + z(s)\vec{i}_z$$

where $\vec{i}_x$, $\vec{i}_y$, $\vec{i}_z$ are unit vectors associated with the cartesian coordinate system x, y and z. Equations $y = y(s)$ and $z = z(s)$ define the closed contour Γ in the y, z plane. The normal vector to the middle surface $\vec{n}$ has two nonzero components

$$\vec{n} = n_y(s)\vec{i}_y + n_z(s)\vec{i}_z \tag{2}$$

The position vector $\vec{R}$ of an arbitrary material point can be written in the form

$$\vec{R} = \vec{r} + \xi\vec{n} \tag{3}$$

Equations (2) and (3) establish the relations between the cartesian coordinates x, y, z and the curvilinear coordinates x, s, ξ. The coordinate ξ lies within the limits

$$-\frac{h(s)}{2} \leq \xi \leq \frac{h(s)}{2}$$

The shell thickness varies along the circumferential direction and is denoted by $h(s)$.

The tangent vector $\vec{t}$, the normal vector $\vec{n}$ and the projection of the position vector $\vec{r}$ on $\vec{t}$ and $\vec{n}$ are expressed in terms of the cartesian and curvilinear coordinates as

$$\vec{t} = \frac{d\vec{r}}{ds} = \frac{dy}{ds}\vec{i}_y + \frac{dz}{ds}\vec{i}_z$$

$$\vec{n} = \vec{t} \times \vec{i}_x = \frac{dz}{ds}\vec{i}_y - \frac{dy}{ds}\vec{i}_z$$

$$r_t = \vec{r} \cdot \vec{t} = y\frac{dy}{ds} + z\frac{dz}{ds}$$
$$r_n = \vec{r} \cdot \vec{n} = y\frac{dz}{ds} - z\frac{dy}{ds}$$

An asymptotical analysis is used to model the slender thin-walled shell as a beam with effective stiffnesses. The method follows an iterative process. The displacement function corresponding to the zeroth-order approximation is obtained first by keeping the leading order terms in the energy functional. A set of successive corrections is added to the displacement function and the associated energy functional is determined. Corrections generating terms of the same order as previously obtained in the energy functional, are kept. The process is terminated when the new contributions do not generate any additional terms of the same order as previously obtained.

Shell Energy Functional

Consider in a $3D$ space the prismatic shell shown in Fig. 2. A curvilinear frame x, s, and ξ is associated with the undeformed shell configuration. Values 1, 2 and 3 denoting x, s, and ξ, respectively are assigned to the curvilinear frame. Throughout this section, Latin superscripts (or subscripts) run from 1 to 3, while Greek superscripts (or subscripts) run from 1 to 2, unless otherwise stated.

The energy density of a $3D$ elastic body is a quadratic form of the strains

$$U = \frac{1}{2}E^{ijkl}\varepsilon_{ij}\varepsilon_{kl}$$

The material properties are expressed by the Hookean tensor E^{ijkl}. Following classical shell formulation (Koiter (1959), and Sanders (1959)) the through-the-thickness stress components σ^{i3} are considerably smaller than the remaining components $\sigma^{\alpha\beta}$ therefore

$$\sigma^{i3} = 0 \tag{4}$$

The strains can be written as

$$\varepsilon_{\alpha\beta} = \gamma_{\alpha\beta} + \xi\rho_{\alpha\beta} \tag{5}$$

where $\gamma_{\alpha\beta}$ and $\rho_{\alpha\beta}$ represent the in-plane strain components and the change in the shell middle surface curvatures , respectively. For a cylindrical shell these are related to the displacement variables by

$$\gamma_{11} = \frac{\partial v_1}{\partial x}$$

$$
\begin{aligned}
2\gamma_{12} &= \frac{\partial v_1}{\partial s} + \frac{\partial v_2}{\partial x} \\
\gamma_{22} &= \frac{\partial v_2}{\partial s} + \frac{v}{R} \\
\rho_{11} &= \frac{\partial^2 v}{\partial x^2} \\
\rho_{12} &= \frac{\partial^2 v}{\partial s \partial x} + \frac{1}{4R}\left(\frac{\partial v_1}{\partial s} - 3\frac{\partial v_2}{\partial x}\right) \\
\rho_{22} &= \frac{\partial^2 v}{\partial s^2} - \frac{\partial}{\partial s}\left(\frac{v_2}{R}\right)
\end{aligned}
\tag{6}
$$

where v_1, v_2 and v represent the displacements in the axial, tangential and normal directions, repectively as shown in Fig. 2. These are related to the displacement components in cartesian coordinates by

$$
\begin{aligned}
v_1 &= u_1 \\
v_2 &= u_2\frac{dy}{ds} + u_3\frac{dz}{ds} \\
v &= u_2\frac{dz}{ds} - u_3\frac{dy}{ds}
\end{aligned}
\tag{7}
$$

where u_1, u_2, and u_3 denote the displacements along the x, y and z coordinates, respectively.

The energy density of the $2D$ elastic body is obtained in terms of $\gamma_{\alpha\beta}$ and $\rho_{\alpha\beta}$ by the following procedure.

The $3D$ energy is first minimized with respect to ϵ_{i3}. This is equivalent to satisfying Eq. (4). The result is

$$
\hat{U} = \min_{\epsilon_{i3}} U = \frac{1}{2} D^{\alpha\beta\gamma\delta}\epsilon_{\alpha\beta}\epsilon_{\gamma\delta} \tag{8}
$$

where $D^{\alpha\beta\gamma\delta}$ represents the components of the $2D$ moduli. The expressions for $D^{\alpha\beta\gamma\delta}$ are given in terms of $E^{\alpha\beta\gamma\delta}$ in the Appendix.

The strain $\epsilon_{\alpha\beta}$ from Eq. (5) is substituted into Eq. (8). After integration of the result over the thickness ξ one obtains the energy of the shell Φ per unit middle surface area

$$
2\Phi = hC^{\alpha\beta\gamma\delta}\gamma_{\alpha\beta}\gamma_{\gamma\delta} + h^2 C_1^{\alpha\beta\gamma\delta}\gamma_{\alpha\beta}\rho_{\gamma\delta} + \frac{h^3}{12} C_2^{\alpha\beta\gamma\delta}\rho_{\alpha\beta}\rho_{\gamma\delta}
$$

where

$$C^{\alpha\beta\gamma\delta} = \frac{1}{h} < D^{\alpha\beta\gamma\delta} >$$

$$C_1^{\alpha\beta\gamma\delta} = \frac{2}{h^2} < D^{\alpha\beta\gamma\delta}\xi >$$

$$C_2^{\alpha\beta\gamma\delta} = \frac{12}{h^3} < D^{\alpha\beta\gamma\delta}\xi^2 >$$

and a function of ξ, say $\alpha(\xi)$, between pointed brackets is defined as an integral through the thickness, viz.,

$$< \alpha >= \int_{-h(s)/2}^{+h(s)/2} \alpha(\xi) d\xi \tag{9}$$

For an applied external loading P_i, the displacement field u_i determining the deformed state is the stationary point of the energy functional

$$I = \int \Phi dx ds - \int P_i u_i dx ds \tag{10}$$

Asymptotical Analysis of the Shell Energy Functional

Zeroth-Order Approximation

Let Δ and E be the order of displacements and stiffness coefficients $C^{\alpha\beta\gamma\delta}$, respectively. Assume that the order of the external forces is

$$P \sim O\left(\frac{E\Delta h}{L^2}\right)$$

This assumption is shown later to be consistent with the equilibrium equations. An alternative would be to assume the order of the external force as some quantity P and derive the order of the displacements as PL^2/Eh from an asymptotical analysis of the energy functional.

For a thin-walled slender beam whose dimensions satisfy Eq. (1) the rate of change of the displacements along the axial direction is much smaller than their rate of change along the circumferential direction. That is, for each displacement component

$$\left|\frac{\partial v_i}{\partial x}\right| << \left|\frac{\partial v_i}{\partial s}\right|$$

Using Eq. (6) and assuming that d is of the same order as R, the order of magnitude of the in-plane strains and curvatures is

$$\gamma_{11} \sim O\left(\frac{\Delta}{L}\right)$$

$$2\gamma_{12} \sim O\left(\frac{\Delta}{d}\right)$$

$$\gamma_{22} \sim O\left(\frac{\Delta}{d}\right)$$

$$\rho_{11} \sim O\left(\frac{\Delta}{L^2}\right)$$

$$\rho_{12} \sim O\left(\frac{\Delta}{d^2}\right)$$

$$\rho_{22} \sim O\left(\frac{\Delta}{d^2}\right)$$

Since γ_{11} and ρ_{11} are much smaller than γ_{12}, γ_{22} and ρ_{12}, ρ_{22}, respectively, their contribution to the elastic energy is neglected.

By keeping the leading order terms in the strain-displacement relationships, Eq. (6) can be written as

$$\begin{aligned} 2\gamma_{12} &= \frac{\partial v_1}{\partial s} \\ \gamma_{22} &= \frac{\partial v_2}{\partial s} + \frac{v}{R} \\ \rho_{12} &= \frac{1}{4R}\frac{\partial v_1}{\partial s} \\ \rho_{22} &= \frac{\partial^2 v}{\partial s^2} - \frac{\partial}{\partial s}\left(\frac{v_2}{R}\right) \end{aligned} \tag{11}$$

The order of magnitude of the shell energy per unit area and the work done by external forces is

$$\Phi \sim O\left(\frac{E\Delta^2 h}{d^2}\right)$$

$$P_i u_i \sim O\left(\frac{E\Delta^2 h}{L^2}\right)$$

Since $P_i u_i << \Phi$, the contribution of external forces is neglected. The energy functional takes the form

$$2I = \int_0^L \oint \{4hC^{1212}(\gamma_{12})^2 + 4hC^{1222}\gamma_{12}\gamma_{22} + hC^{2222}(\gamma_{22})^2 + 4h^2C_1^{1212}\gamma_{12}\rho_{12}$$
$$+2h^2C_1^{1222}\gamma_{12}\rho_{22} + 2h^2C_1^{2212}\gamma_{22}\rho_{12} + h^2C_1^{2222}\gamma_{22}\rho_{22}$$
$$+\frac{h^3}{3}C_2^{1212}(\rho_{12})^2 + \frac{h^3}{3}C_2^{1222}\rho_{12}\rho_{22} + \frac{h^3}{12}C_2^{2222}(\rho_{22})^2\}dsdx \tag{12}$$

The integrand in Eq. (12) is a positive quadratic form, therefore the minimum of the functional is reached by functions v, v_1, and v_2 for which $\gamma_{12} = \gamma_{22} = \rho_{12} = \rho_{22} = 0$. From Eq. (11) this corresponds to

$$\frac{\partial v_1}{\partial s} = 0 \tag{13}$$

$$\frac{\partial v_2}{\partial s} + \frac{v}{R} = 0 \tag{14}$$

$$\frac{\partial^2 v}{\partial s^2} - \frac{\partial}{\partial s}\left(\frac{v_2}{R}\right) = 0 \tag{15}$$

The function v in Eqs. (14) and (15) should be single valued, i. e.

$$\overline{\left(\frac{\partial v}{\partial s}\right)} \equiv \frac{1}{l}\oint \frac{\partial v}{\partial s}ds = 0 \tag{16}$$

The integral in Eq. (16) is performed along the cross sectional mid-plane closed contour Γ. The length of contour Γ is denoted by l. The bar in Eq. (16) and in the subsequent derivation denotes averaging along the closed contour Γ.

Equation (13) implies that v_1 is a function of x only, i.e.

$$v_1 = U_1(x) \tag{17}$$

Integrate Eq. (15) to get

$$\frac{\partial v}{\partial s} - \frac{v_2}{R} = -\varphi(x) \tag{18}$$

where $\varphi(x)$ is an arbitrary function which is shown later to represent the cross sectional rotation about the x-axis. From Eq. (16) and (18), one obtains the relation between $\varphi(x)$ and v_2.

$$\varphi(x) = \overline{\left(\frac{v_2}{R}\right)}$$

Substitute v from Eq. (14) into Eq. (18), to get the following second-order differential equation for v_2

$$\frac{\partial}{\partial s}(R\frac{\partial v_2}{\partial s}) + \frac{v_2}{R} = \varphi(x) \tag{19}$$

To solve this equation, one has to recall the relations between the radius of curvature R and the components $y(s)$ and $z(s)$ of the position vector associated with contour Γ

$$\frac{d^2z}{ds^2} = \frac{1}{R}\frac{dy}{ds}$$

$$\frac{d^2y}{ds^2} = -\frac{1}{R}\frac{dz}{ds} \tag{20}$$

It follows from Eq. (20) that $\frac{dy}{ds}$ and $\frac{dz}{ds}$ are solutions of the homogeneous form of Eq. (19) and $v_2 = \varphi(x)r_n$ is its particular solution. The general solution is therefore given by

$$v_2 = U_2(x)\frac{dy}{ds} + U_3(x)\frac{dz}{ds} + \varphi(x)r_n \tag{21}$$

where U_2 and U_3 are arbitrary functions of x. Substitute from Eq. (21) into Eq. (14) to get

$$v = U_2(x)\frac{dz}{ds} - U_3(x)\frac{dy}{ds} - \varphi(x)r_t \tag{22}$$

Equations (17), (21) and (22) represent the curvilinear displacement field that minimizes the zeroth order approximation of the shell energy. Using Eq. (7) the curvilinear displacement field is written in Cartesian coordinates as

$$u_1 = U_1(x)$$

$$u_2 = U_2(x) - z\varphi(x)$$

$$u_3 = U_3(x) + y\varphi(x)$$

The variables $U_1(x), U_2(x)$ and $U_3(x)$ represent the average cross-sectional translation while $\varphi(x)$ the cross-sectional rotation normally referred to in beam theory as the torsional rotation. This displacement field corresponds to the zeroth-order approximation and does not include bending behavior. For a centroidal coordinate system $U_1(x)$, $U_2(x)$, $U_3(x)$ and $\varphi(x)$ can be expressed as

$$U_1(x) = \overline{u_1}$$

$$U_2(x) = \overline{u_2}$$

$$U_3(x) = \overline{u_3}$$

$$\varphi(x) = \frac{\overline{(\vec{u} \cdot \vec{t})}}{\overline{r_n}}$$

First-Order Approximation

A first-order approximation can be constructed by rewriting the displacement field in Eqs. (17), (21) and (22) in the form

$$\begin{aligned} v_1 &= U_1(x) + w_1(s,x) \\ v_2 &= U_2(x)\frac{dy}{ds} + U_3(x)\frac{dz}{ds} + \varphi(x) r_n + w_2(s,x) \\ v &= U_2(x)\frac{dz}{ds} - U_3(x)\frac{dy}{ds} - \varphi(x) r_t + w(s,x) \end{aligned} \tag{23}$$

where w_1, w_2 and w can be regarded as correction functions to be determined based on their contributions to the energy functional.

Substitute Eq. (23) into Eq. (6) to obtain the strains and curvatures in terms of the displacement corrections

$$\begin{aligned} \gamma_{11} &= \mathring{\gamma}_{11} + \frac{\partial w_1}{\partial x} \\ 2\gamma_{12} &= 2\mathring{\gamma}_{12} + \frac{\partial w_2}{\partial x} + 2\hat{\gamma}_{12} \quad , \quad 2\hat{\gamma}_{12} = \frac{\partial w_1}{\partial s} \\ \gamma_{22} &= \mathring{\gamma}_{22} + \hat{\gamma}_{22} \quad , \quad \hat{\gamma}_{22} = \frac{\partial w_2}{\partial s} + \frac{w}{R} \\ \rho_{11} &= \mathring{\rho}_{11} + \frac{\partial^2 w}{\partial x^2} \\ \rho_{12} &= \mathring{\rho}_{12} + \frac{\partial^2 w}{\partial s \partial x} - \frac{3}{4R}\frac{\partial w_2}{\partial x} + \hat{\rho}_{12} \quad , \quad \hat{\rho}_{12} = \frac{1}{4R}\frac{\partial w_1}{\partial s} \\ \rho_{22} &= \mathring{\rho}_{22} + \hat{\rho}_{22} \quad , \quad \hat{\rho}_{22} = \frac{\partial^2 w}{\partial s^2} - \frac{\partial}{\partial s}\left(\frac{w_2}{R}\right) \end{aligned} \tag{24}$$

where $\gamma^\circ{}_{\alpha\beta}$ and $\rho^\circ{}_{\alpha\beta}$ are the strains and curvatures corresponding to the zeroth-order approximation. These are expressed as

$$\begin{aligned} \mathring{\gamma}_{11} &= U_1'(x) \\ 2\mathring{\gamma}_{12} &= U_2'(x)\frac{dy}{ds} + U_3'(x)\frac{dz}{ds} + \varphi'(x) r_n \\ \mathring{\gamma}_{22} &= 0 \end{aligned}$$

$$\mathring{\rho}_{11} = U_2''(x)\frac{dz}{ds} - U_3''(x)\frac{dy}{ds} - \varphi''(x)r_t \tag{25}$$

$$\mathring{\rho}_{12} = \frac{1}{4R}\left[U_2'(x)\frac{dy}{ds} + U_3'(x)\frac{dz}{ds} + \varphi'(x)r_n\right] - \varphi'(x)$$

$$\mathring{\rho}_{22} = 0$$

The prime in Eq. (25) denotes differentiation with respect to x. The order of w_i is $(\frac{\Delta d}{L})$. Among the new terms introduced by the function w_i the leading ones are denoted by superscript $\mathring{}$ in Eq. (24). By keeping their contribution over the other terms, the energy functional can be represented by

$$\Phi(\mathring{\gamma}_{11}, 2\mathring{\gamma}_{12} + 2\hat{\gamma}_{12}, \hat{\gamma}_{22}, 0, \hat{\rho}_{12}, \hat{\rho}_{22})$$

where terms of order $(\frac{\Delta^2 h}{L^2 d})$ or smaller such as

$$h\mathring{\rho}_{11}\hat{\gamma}_{12}\,,\; h\mathring{\rho}_{11}\hat{\gamma}_{22}\,,\; h^2\mathring{\rho}_{11}\hat{\rho}_{12}\,,\; h^2\mathring{\rho}_{11}\hat{\rho}_{22}$$

$$h\mathring{\rho}_{12}\hat{\gamma}_{12}\,,\; h\mathring{\rho}_{12}\hat{\gamma}_{22}\,,\; h^2\mathring{\rho}_{12}\hat{\rho}_{12}\,,\; h^2\mathring{\rho}_{12}\hat{\rho}_{22}$$

are neglected in comparison with the following terms

$$\mathring{\gamma}_{11}\hat{\gamma}_{12}\,,\; \mathring{\gamma}_{11}\hat{\gamma}_{22}\,,\; \mathring{\gamma}_{12}\hat{\gamma}_{12}\,,\; \mathring{\gamma}_{12}\hat{\gamma}_{22}$$

of order $(\frac{\Delta^2}{L^2})$. Similarly, the contribution of the work done by external forces, $P_i w_i$, is neglected since its order is $\left(Eh\frac{\Delta^2}{L^2}(\frac{d}{L})\right)$ in comparison with the order of the remaining terms in the energy functional $\left(Eh\frac{\Delta^2}{L^2}\right)$. Therefore in order to determine the functions w_i one has to minimize the functional

$$\oint \Phi(\mathring{\gamma}_{11}, 2\mathring{\gamma}_{12} + 2\hat{\gamma}_{12}, \hat{\gamma}_{22}, 0, \hat{\rho}_{12}, \hat{\rho}_{22})\, ds$$

If the rigid body motion is suppressed the solution is unique. The terms $\hat{\rho}_{12}$, $\hat{\rho}_{22}$ are essential to the uniqueness of the solution; however, their contribution to the energy is of order $\left(Eh\frac{\Delta^2}{L^2}(\frac{h}{d})\right)$ and is consequently dropped. This aspect is discussed by Berdichevsky and Misiura (1991) with regard to the accuracy of classical shell theory. The shell energy can therefore be represented by

$$I = \int_0^L \oint \Phi(\mathring{\gamma}_{11}, 2\mathring{\gamma}_{12} + 2\hat{\gamma}_{12}, \hat{\gamma}_{22}, 0, 0, 0)\, ds dx \tag{26}$$

It is worth noting that the bending contribution does not appear in Eq. (26). That is, to the first order approximation the shell energy corresponds to a membrane state.

The first variation of the energy functional is

$$\delta I = \int_0^L \oint \left\{ \frac{\partial \Phi}{\partial (2\gamma_{12})} \delta \left(\frac{\partial w_1}{\partial s} \right) + \frac{\partial \Phi}{\partial \gamma_{22}} \delta \left(\frac{\partial w_2}{\partial s} + \frac{w}{R} \right) \right\} ds dx \tag{27}$$

Equation (27) can be written in terms of the shear flow N_{12} and hoop stress resultant N_{22} by recalling that $N_{12} = \frac{\partial \Phi}{\partial (2\gamma_{12})}$ and $N_{22} = \frac{\partial \Phi}{\partial \gamma_{22}}$. The result is

$$\delta I = \int_0^L \oint \left\{ N_{12} \frac{\partial (\delta w_1)}{\partial s} + N_{22} \left(\frac{\partial (\delta w_2)}{\partial s} + \frac{1}{R} \delta w \right) \right\} ds dx$$

Set the first variation of the energy to zero, to obtain the following

$$\frac{\partial N_{12}}{\partial s} = 0$$

$$\frac{\partial N_{22}}{\partial s} = 0$$

$$\frac{N_{22}}{R} = 0$$

which result in

$$N_{12} = \text{constant} \tag{28}$$

and

$$N_{22} = 0 \tag{29}$$

This is similar to the classical solution of constant shear flow and vanishing hoop stress. By setting N_{22} to zero the energy density is expressed in terms of γ_{11} and γ_{12} only

$$2\Phi_1 = \min_{\gamma_{22}} 2\Phi = A(s)(\gamma_{11})^2 + 2B(s)\gamma_{11}\gamma_{12} + C(s)(\gamma_{12})^2 \tag{30}$$

The variables $A(s)$, $B(s)$ and $C(s)$ represent the axial, coupling and shear stiffnesses, respectively. They are defined in terms of the $2D$ shell moduli in the Appendix.

Equation (30) indicates that, to the first order, the energy density function is independent of functions w_2 and w. That is the in-plane warping contribution to the shell energy is negligible. The function w_1 however, can be determined from Eqs. (28) and (30) and by enforcing the condition on w_1 to be single valued as follows

$$N_{12} = \frac{\partial \Phi_1}{\partial (2\gamma_{12})} = \frac{1}{2} \left(B(s)\gamma_{11} + C(s)\gamma_{12} \right) = \text{constant} \tag{31}$$

Substitute the leading terms from Eqs. (24) and (25) into Eq. (31) to get

$$\frac{1}{2}BU_1'(x) + \frac{1}{4}C\left(U_2'(x)\frac{dy}{ds} + U_3'(x)\frac{dz}{dx} + \varphi'(x)r_n(s) + \frac{\partial w_1}{\partial s}\right) = \text{constant} \qquad (32)$$

In deriving Eq. (32) the term $B\frac{\partial w_1}{\partial x}$ has been neglected in comparison with $\frac{1}{2}C\frac{\partial w_1}{\partial s}$. This is possible if $|B|$ is less or of the same order of magnitude as C. For the case when $|B| >> C$ additional investigation is needed. Since the elastic energy is positive definite, $B^2 \leq AC$, and B could be greater than C only if $A >> C$. In practical laminated composite designs $|B| < C$, as the shear stiffness is greater than the extension-shear coupling.

Equation (32) is a first-order ordinary differential equation in w_1. The value of the constant in the right hand side of Eq. (32) can be found from the single value condition of function w_1:

$$\overline{\left(\frac{\partial w_1}{\partial s}\right)} \equiv \frac{1}{l}\oint \frac{\partial w_1}{\partial s}ds = 0$$

The solution of Eq. (32) is determined within an arbitrary function of x. This function can be specified from various conditions. Each one yields a specific interpretation of the variable U_1. For example if $\overline{w_1} = 0$ the variable $U_1 = \overline{v_1}$ according to Eq. (23). The choice of these conditions does not affect the final form of the $1D$ beam theory and therefore will not be specified in this formulation. The result is the following simple analytical solution of Eq. (32)

$$w_1 = -yU_2'(x) - zU_3'(x) + G(s)\varphi'(x) + g_1(s)U_1'(x) \qquad (33)$$

where

$$G(s) = \int_0^s \left[\frac{2A_e}{l\,\bar{c}}c(\tau) - r_n(\tau)\right]d\tau$$

$$g_1(s) = \int_0^s \left[b(\tau) - \frac{\bar{b}}{\bar{c}}c(\tau)\right]d\tau$$

$$b(s) = -2\frac{B(s)}{C(s)} \qquad c(s) = \frac{1}{C(s)} \qquad A_e = \frac{l}{2}\overline{r_n} \qquad (34)$$

The area enclosed by contour Γ is denoted by A_e in Eq. (34).

The displacement field corresponding to the first correction is obtained by substituting Eq. (33) into Eq. (23) and dropping w_2 and w since their contribution to

the shell energy is negligible compared to w_1. The result referred to as first-order approximation is given by

$$v_1 = U_1(x) - y(s)U_2'(x) - z(s)U_3'(x) + G(s)\varphi'(x) + g_1(s)U_1'(x)$$

$$v_2 = U_2(x)\frac{dy}{ds} + U_3(x)\frac{dz}{ds} + \varphi(x)r_n$$

$$v = U_2(x)\frac{dz}{ds} - U_3(x)\frac{dy}{ds} - \varphi(x)r_t$$

Displacement Field

The displacement field corresponding to the next correction is found in the same way. A third correction can also be performed. However, subsequent corrections yield only smaller terms, as shown in Badir (1992), and the displacement field converges to the following expression

$$\begin{aligned} v_1 &= U_1(x) - y(s)U_2'(x) - z(s)U_3'(x) + G(s)\varphi'(x) \\ &\quad + g_1(s)U_1'(x) + g_2(s)U_2''(x) + g_3(s)U_3''(x) \end{aligned}$$

$$v_2 = U_2(x)\frac{dy}{ds} + U_3(x)\frac{dz}{ds} + \varphi(x)r_n \qquad (35)$$

$$v = U_2(x)\frac{dz}{ds} - U_3(x)\frac{dy}{ds} - \varphi(x)r_t$$

where

$$g_2(s) = -\int_0^s \left[b(\tau)y(\tau) - \frac{\overline{by}}{\overline{c}}c(\tau)\right]d\tau$$

$$g_3(s) = -\int_0^s \left[b(\tau)z(\tau) - \frac{\overline{bz}}{\overline{c}}c(\tau)\right]d\tau \qquad (36)$$

It is seen from expressions (34) and (36) that $G(s)$, $g_1(s)$, $g_2(s)$, and $g_3(s)$ are single-valued functions, that is

$$G(0) = G(l) = g_1(0) = g_1(l) = g_2(0) = g_2(l) = g_3(0) = g_3(l) = 0$$

The expressions for the displacements v_2, v and the first four terms in v_1 are analogous to the classical theory of extension, bending and torsion of beams. The additional terms $g_1(s)U_1'$, $g_2(s)U_2''$ and $g_3(s)U_3''$ in the expression of v_1 in Eq. (35) represent warping due to axial strain and bending. These new terms emerge naturally in addition to the classical torsional related warping $G(s)\varphi'$. They are strongly

influenced by the material's anisotropy, and vanish for materials that are either orthotropic or whose properties are antisymmetric relative to the shell middle surface. These out-of-plane warping functions were first derived by Armanios *et al.* (1991) for laminated composites.

The contribution of out-of-plane warping was considered recently by Kosmatka (1991). Local in-plane deformations and out-of-plane warping of the cross section were expressed in terms of unknown functions. These functions were assumed to be proportional to the axial strain, bending curvature and twist rate within the cross section and were determined using a finite element modeling. In the present formulation, the out-of-plane warping is shown to be proportional to the axial strain, bending curvature and torsion twist rate. The functions associated with each physical behavior are expressed in closed-form by $g_1(s)$ for the axial strain, $g_2(s)$ and $g_3(s)$ for the bending curvatures and $G(s)$ for the torsion twist rate.

Strain Field

The strain field is obtained by substituting Eq. (35) into Eq. (6) and neglecting terms of smaller order in the shell energy. The result is

$$\gamma_{11} = U_1'(x) - y(s)U_2''(x) - z(s)U_3''(x)$$

$$\begin{aligned} 2\gamma_{12} &= \frac{2A_e}{l\overline{c}}c(s)\varphi' + \left[b(s) - \frac{\overline{b}}{\overline{c}}c(s)\right]U_1' \\ &\quad - \left[b(s)y(s) - \frac{\overline{by}}{\overline{c}}c(s)\right]U_2'' \\ &\quad - \left[b(s)z(s) - \frac{\overline{bz}}{\overline{c}}c(s)\right]U_3'' \end{aligned} \tag{37}$$

$$\gamma_{22} = 0$$

It is worth noting that the vanishing of hoop stress resultant in Eq. (29) and hoop strain in Eq. (37) should be interpreted as negligible contribution relative to other parameters. The longitudinal strain γ_{11} is a linear function of y and z. This result was adopted as an assumption in the work of Libove (1988).

In deriving Eq. (37), higher order terms associated with $G\varphi''$ in the energy functional have been neglected in comparison with $C\left(\frac{A_e}{l\overline{c}}c\varphi'\right)^2$ as shown in Badir (1992). This is possible if the following inequalities are satisfied

$$\frac{A}{C}\left(\frac{d}{L}\right) << 1 \qquad \frac{B}{C}\left(\frac{d}{L}\right) << 1$$

Constitutive Relationships

Substitute Eq. (37) in the energy density, Eq. (30), and integrate over s to get the energy of $1D$ beam theory

$$I = \int_0^L \Phi_2 dx - \int P_i u_i dx ds \tag{38}$$

where

$$\begin{aligned} \Phi_2 \;=\; & \frac{1}{2}\left[C_{11}(U_1')^2 + C_{22}(\varphi')^2 + C_{33}(U_3'')^2 + C_{44}(U_2'')^2\right] \\ & + C_{12}U_1'\varphi' + C_{13}U_1'U_3'' + C_{14}U_1'U_2'' \\ & + C_{23}\varphi'U_3'' + C_{24}\varphi'U_2'' + C_{34}U_2''U_3'' \end{aligned} \tag{39}$$

Explicit expressions for the stiffness coefficients C_{ij} $(i, j = 1, 4)$ are given in the Appendix.

The constitutive relationships can be written in terms of stress resultants and kinematic variables by differentiating Eq. (39) with respect to the associated kinematic variable or by relating the traction T, torsional moment M_x, and bending moments M_y and M_z to the shear flow and axial stress as follows

$$\begin{aligned} T &= \frac{\partial \Phi_2}{\partial U_1'} = \oint \int \sigma_{11} d\xi ds = \oint N_{11} ds \\ M_x &= \frac{\partial \Phi_2}{\partial \varphi'} = \oint \int \sigma_{12} r_n(s) d\xi ds = \oint N_{12} r_n(s) ds \\ M_y &= \frac{\partial \Phi_2}{\partial U_3''} = -\oint \int \sigma_{11} z d\xi ds = -\oint N_{11} z(s) ds \\ M_z &= \frac{\partial \Phi_2}{\partial U_2''} = -\oint \int \sigma_{11} y d\xi ds = -\oint N_{11} y(s) ds \end{aligned} \tag{40}$$

The shear flow N_{12} is derived from the energy density in Eq. (31) and the axial stress resultant N_{11} is given by

$$N_{11} = \frac{\partial \Phi_1}{\partial \gamma_{11}} = A(s)\gamma_{11} + B(s)\gamma_{12} \tag{41}$$

and the associated axial and shear stresses are uniform through the wall thickness.

Substitute Eq. (37) into Eqs. (31) and (41) and use Eq. (40) to get

$$\begin{Bmatrix} T \\ M_x \\ M_y \\ M_z \end{Bmatrix} = \begin{bmatrix} C_{11} & C_{12} & C_{13} & C_{14} \\ C_{12} & C_{22} & C_{23} & C_{24} \\ C_{13} & C_{23} & C_{33} & C_{34} \\ C_{14} & C_{24} & C_{34} & C_{44} \end{bmatrix} \begin{Bmatrix} U_1' \\ \varphi' \\ U_3'' \\ U_2'' \end{Bmatrix} \tag{42}$$

Equilibrium Equations

The equilibrium equations can be derived by substituting the displacement field in Eq. (35) into the energy functional in Eq. (10) and using the principle of minimum total potential energy to get

$$\begin{aligned} T' + \oint P_x ds &= 0 \\ M_x' + \oint (P_x y - P_y z) ds &= 0 \\ M_y'' + (\oint P_x z ds)' + \oint P_z ds &= 0 \\ M_z'' + (\oint P_x y ds)' + \oint P_y ds &= 0 \end{aligned} \tag{43}$$

where P_x, P_y and P_z are surface tractions along the x, y and z directions, respectively.

One of the member of each of the following four pairs must be prescribed at the beam ends :

$$T \text{ or } U_1,\ M_x \text{ or } \varphi,\ M_y \text{ or } U_3',\ \text{and } M_z \text{ or } U_2' \tag{44}$$

SUMMARY OF GOVERNING EQUATIONS

The development presented in this work encompasses five equations. The first, is the displacement field given in Eq. (35). Its functional form was determined based on an asymptotical expansion of shell energy. The associated strain field is given in Eq. (37) and the stress resultants in Eqs. (31), (40) and (41). The fourth, are the constitutive relationships in Eq. (42) with the stiffness coefficients expressed as integrals of material properties and cross sectional geometry in Eq. (56) of the Appendix. Finally the equilibrium equations and boundary conditions are given in Eq. (43) and (44), respectively.

In the present development the determination of the displacement field is essential in obtaining accurate expressions for the beam stiffnesses. A comparison of the derived displacement field with results obtained by previous investigators is presented in the following section.

COMPARISON OF DISPLACEMENT FIELDS

The pioneering work of Reissner and Tsai (1972) is based on developing an exact solution to the governing equilibrium, compatibility and constitutive relationships of shell theory. Closed as well as open cross-sections were considered. The derived constitutive relationships are similar to Eq. (42). However, the authors left to the reader the derivation of the explicit expressions for the stiffness coefficients. This may be the reason for their work to have been overlooked. These expressions are important in identifying the parameters controlling the behavior and in performing parametric design studies. Furthermore, the explicit form of the displacement field helps evaluate and understand predictions of other analytical and numerical models.

A number of assumptions were adopted in Reissner and Tsai's development regarding material properties such as neglecting the coupling between in-plane strains and curvatures which can be significant in anisotropic materials. It is important to assess the influence of these assumptions on the accuracy. This has been done in the present work by using an asymptotical expansion of the shell energy and proving that the coupling and curvatures contributions to the energy are small in comparison with the in-plane contribution.

Mansfield and Sobey (1979) and Libove (1988) obtained the beam flexibilities relating the stretching, twisting and bending deformations to the applied axial load, torsional and bending moments for a special origin and axes orientation. They adopted the assumptions of a negligible hoop stress resultant N_{ss} and a membrane state in the thin-walled beam section. Although they did not refer to the work of Reissner and Tsai (1972), their stiffnesses coincide for the special case outlined in Reissner and Tsai (1972). This special case refers to the one where the classical assumptions of neglecting shear and hoop stresses and considering the shear flow to be constant is adopted. However, one has to carry out the details to show this fact.

The work of Rehfield (1985) has been used in a number of composite applications. Rehfield's displacement field is of the form

$$\begin{aligned} u_1 &= U_1(x) - y(s)\left[U_2'(x) - 2\gamma_{xy}(x)\right] - z(s)\left[U_3'(x) - 2\gamma_{xz}(x)\right] + g(s,x) \\ u_2 &= U_2(x) - z(s)\varphi(x) \\ u_3 &= U_3(x) + y(s)\varphi(x) \end{aligned} \tag{45}$$

where γ_{xx} and γ_{xy} are the transverse shear strains. The warping function $g(s,x)$ is given as

$$g(s,x) = \bar{G}(s)\varphi'(x) \tag{46}$$

with

$$\bar{G}(s) = 2A_e\frac{s}{l} - \int_0^s r_n(\tau)d\tau \tag{47}$$

A comparison of the displacement fields in Eq. (35) and (45) shows that the warping function in Rehfield's formulation comprises the torsional-related contribution but does not include explicit terms that express the bending-related warping. The torsional warping function $G(s)$ in Eq. (34) is different from the function in Eq. (47). The two expressions coincide when c = constant that is, when the wall stiffness and thickness are uniform along the cross section circumference.

The torsional warping function in Eq. (47) was modified by Atilgan (1989) and Rehfield and Atilgan (1989) as

$$\hat{G}(s) = \int_0^s \left[\frac{2A_e}{l\,\overline{c_1}} c_1 - \tau_n(\tau)\right] d\tau \tag{48}$$

where

$$c_1 = \frac{1}{A'_{66} - \frac{(A'_{16})^2}{A'_{11}}} \tag{49}$$

and

$$\begin{bmatrix} A'_{11} & A'_{16} \\ A'_{16} & A'_{66} \end{bmatrix} = \begin{bmatrix} A_{11} - \frac{(A_{12})^2}{A_{22}} & A_{16} - \frac{A_{12}A_{26}}{A_{22}} \\ A_{16} - \frac{A_{12}A_{26}}{A_{22}} & A_{66} - \frac{(A_{26})^2}{A_{22}} \end{bmatrix} \tag{50}$$

The A_{ij} in Eq. (50) are the in-plane stiffnesses of Classical Lamination Theory (Jones (1975) and Vinson and Sierakowski (1987)). They are related to the modulus tensor by

$$A_{11} =< E^{1111} > \quad , \quad A_{12} =< E^{1122} > \quad , \quad A_{22} =< E^{2222} >$$

$$A_{16} =< E^{1112} > \quad , \quad A_{26} =< E^{1222} > \quad , \quad A_{66} =< E^{1212} >$$

A comparison of the modified torsional warping function in Eq. (48) and $G(s)$ in Eq. (34) shows that they coincide for laminates with no extension-shear coupling ($< D^{1112} >=< D^{1222} >= 0$, in Eq. (54) of the Appendix). For the case where the through-the-thickness contribution is neglected in Eq. (54), this reduces to $A_{16} = A_{26} = 0$.

The warping function obtained by Smith and Chopra (1990, 1991) for composite box-beams is identical to the expression of Rehfield and Atilgan (1989) and Atilgan (1989) given in Eqs. (46) and (48).

An assessment of all the previous warping expressions can be made by checking whether they reduce to the exact expression for isotropic materials (see, for example,

Megson (1990))

$$\bar{\tilde{G}}(s) = \int_0^s \left[\frac{2A_e}{l\,\overline{c_2}} c_2 - r_n(\tau)\right] d\tau \tag{51}$$

with

$$c_2 = \frac{1}{\mu h(s)}$$

where μ is the shear modulus.

For isotropic materials the in-plane coupling b is zero and consequently g_1, g_2 and g_3 in Eqs. (34) and (36) vanish. That is the warping is torsion-related and reduces to $G(s)\varphi'$. Moreover, the shear parameter c is equal to $\frac{1}{4\mu h(s)}$ and the expressions for $G(s)$ and $\bar{\tilde{G}}(s)$ in Eqs. (34) and (51) coincide.

Rehfield's warping function in Eq. (47) coincides with Eq. (51) when the material properties and the thickness are uniform along the wall circumference. Atilgan's (1989), Rehfield and Atilgan's (1989), and Smith and Chopra's (1991) formulations reduce to Eq. (51) for isotropic materials.

APPLICATIONS

Two special layups: the circumferentially uniform stiffness (CUS) and circumferentially asymmetric stiffness (CAS) have been considered by Atilgan (1989), Rehfield and Atilgan (1989), Hodges *et al.* (1989), Rehfield *et al.* (1990), Chandra *et al.* (1990), and Smith and Chopra (1990, 1991).

CUS Configuration

This configuration produces extension-twist coupling. The axial, coupling and in-plane stiffnesses A, B, and C given in Eq. (53) of the Appendix are constant throughout the cross section, and hence the name circumferentially uniform stiffness (CUS) was adopted by Atilgan (1989), Rehfield and Atilgan (1989), Hodges *et al.* (1989), and Rehfield *et al.* (1990). For a box-beam, the ply lay-ups on opposite sides are of reversed orientation, and hence the name antisymmetric configuration was adopted by Chandra *et al.* (1990), and Smith and Chopra (1990,1991).

Since A, B, and C are constants, the stiffness matrix in Eq. (42), for a centroidal

coordinate system, reduces to

$$\begin{bmatrix} C_{11} & C_{12} & 0 & 0 \\ C_{12} & C_{22} & 0 & 0 \\ 0 & 0 & C_{33} & 0 \\ 0 & 0 & 0 & C_{44} \end{bmatrix}$$

The nonzero stiffness coefficients are given by

$$\begin{aligned} C_{11} &= Al \\ C_{12} &= BA_e \\ C_{22} &= \frac{C}{l} A_e^2 \\ C_{33} &= A \oint z^2 ds - \frac{B^2}{C} \oint z^2 ds \\ C_{44} &= A \oint y^2 ds - \frac{B^2}{C} \oint y^2 ds \end{aligned} \tag{52}$$

For such a case the out-of-plane warping due to axial strain vanishes and g_1 does not affect the response.

CAS Configuration

This configuration produces bending-twist coupling. The stiffness A is constant throughout the cross section. For a box beam, the coupling stiffness, B in opposite members is of opposite sign and hence the name circumferentially asymmetric stiffness (CAS) was adopted by Atilgan(1989), Rehfield and Atilgan(1989), Hodges *et al.*(1989), and Rehfield *et al.*(1990). For a box-beam, the ply lay-ups along the horizontal members are mirror images, and hence the name symmetric configuration was adopted by Chandra *et al.*(1990), and Smith and Chopra(1990,1991). The stiffness C in opposite members is equal. The stiffness matrix, for a centroidal system of axes, reduces to

$$\begin{bmatrix} C_{11} & 0 & 0 & 0 \\ 0 & C_{22} & C_{23} & 0 \\ 0 & C_{23} & C_{33} & 0 \\ 0 & 0 & 0 & C_{44} \end{bmatrix}$$

The nonzero stiffness coefficients are expressed by

$$C_{11} = Al - 2\frac{B_t^2}{C_t} d$$

Table 1: Properties of T300/5208 Graphite/Epoxy

$E_{11} = 21.3$ Msi
$E_{22} = E_{33} = 1.6$ Msi
$G_{12} = G_{13} = 0.9$ Msi
$G_{23} = 0.7$ Msi
$\nu_{12} = \nu_{13} = 0.28$
$\nu_{23} = 0.5$

$$C_{22} = \frac{C_t}{2\left[d + a\left(\frac{C_t}{C_v}\right)\right]} A_e^2$$

$$C_{23} = \frac{B_t}{2\left[d + a\left(\frac{C_t}{C_v}\right)\right]} A_e^2$$

$$C_{33} = A \oint z^2 ds - \frac{B_t^2}{2C_t} \left\{ a - \frac{A_e}{\left[d + a\left(\frac{C_t}{C_v}\right)\right]} \right\} A_e$$

$$C_{44} = A \oint y^2 ds - \frac{B_t^2 d^3}{6C_t}$$

Subscripts t and v denote top and vertical members, respectively. The box width and height are denoted by d and a, respectively. For the CAS configuration and with reference to the Cartesian coordinate system in Fig. 1, bending about the y-axis is coupled with torsion while extension and bending about the z-axis are decoupled.

In order to assess the accuracy of the predictions the present theory is applied to the box beam studied by Hodges *et al.* (1989). The cross sectional configuration is shown in Fig. 3 and the material properties in Table 1.

Flexibility Coefficients

A comparison of the flexibility coefficients S_{ij} with the predictions from two models is provided in Table 2. The flexibility coefficients S_{ij} are obtained by inverting the 4×4 matrix in Eq. (42). The NABSA (Nonhomogeneous Anisotropic Beam Section Analysis) is a finite element model based on an extension of the work of Giavotto

Table 2: Comparison of Flexibility Coefficients of NABSA, TAIL and Present (lb,in units)

Flexibility	NABSA	PRESENT	% Diff.	TAIL	% Diff.
$S_{11} \times 10^5$	0.143883	0.14491	+0.7	0.14491	+0.7
$S_{22} \times 10^4$	0.312145	0.32364	+3.6	0.32364	+3.6
$S_{12} \times 10^5$	−0.417841	−0.43010	+2.9	−0.43010	+2.9
$S_{33} \times 10^4$	0.183684	0.1886	+2.6	0.17294	−5.8
$S_{44} \times 10^5$	0.614311	0.63429	+3.2	0.50157	−18.4

Table 3: Geometry and Mechanical Properties of Thin-Walled Beam with $[+12]_4$ CUS square cross-section

Length = 24.0 in.	$E_{11} = E_{22} = E_{33} = 11.65$ Msi
Width = depth = 1.17 in.	$G_{12} = G_{13} = 0.82,\ G_{23} = 0.7$ Msi
Ply thickness = 0.0075 in.	$\nu_{12} = \nu_{13} = 0.05,\ \nu_{23} = 0.3$

et al.(1983). In this model all possible types of warping are accounted for. The TAIL model is based on the theory of Rehfield (1985) while neglecting the restrained torsional warping. The predictions of the NABSA and TAIL models are provided by Hodges *et al.*(1989). The percentage differences appearing in Table 2 are relative to the NABSA predictions. The present theory is in good agreement with NABSA. Its predictions show a difference ranging from +0.7 to +3.6 percent while those based on Rehfield's theory (1985) range from +3.6 to −18.4 percent.

The present theory is applied to the prediction of the tip deformation in a cantilevered beam made of Graphite/Epoxy and subjected to different types of loading. The beam has a CUS square cross section with $[+12]_4$ lay-up. The geometry and mechanical properties are given in Table 3. Comparison of results with the MSC/NASTRAN finite element analysis of Nixon (1989) is provided in Table 4. The MSC/NASTRAN analysis is based on a $2D$ plate model. The predictions of the present theory range from +1.7 to −0.7 percent difference relative to the finite ele-

Table 4: MSC/NASTRAN and Present Solutions for a CUS Cantilevered Beam with $[+12]_4$ Layups Subjected to Various Tip Load Cases

Tip Load	Tip Deformation			% Diff.
		NASTRAN	Present	
Axial Force (100 lb)	Axial Disp. :	0.002189 in.	0.002202 in.	+0.6 %
Axial Force (100 lb)	Twist :	0.3178 deg.	0.32325 deg.	+1.7 %
Torsional Moment (100 lb·in)	Twist :	2.959 deg.	2.998 deg.	+1.32 %
Transverse Force (100 lb)	Deflection :	1.866 in.	1.853 in.	−0.7 %

Table 5: Cantilever Geometry and Properties

Width = 0.953 in.	$E_{11} = 20.59$ Msi, $E_{22} = E_{33} = 1.42$ Msi
Depth = 0.53 in.	$G_{12} = G_{13} = 0.87$ Msi, $G_{23} = 0.7$ Msi
Ply thickness = 0.005 in.	$\nu_{12} = \nu_{13} = 0.42$, $\nu_{23} = 0.5$

ment results.

For a CUS configuration, the extension-torsional response is decoupled from bending. Since C is constant and g_1 does not affect the stiffness coefficients, the flexibility coefficients controlling extension and twist response, S_{11}, S_{12} and S_{22} coincide with those of Atilgan (1989), and Rehfield and Atilgan (1989). As a consequence, the axial displacement and twist angle predictions coincide. However, the lateral deflection under transverse load differs. The tip lateral deflection predicted using the theory of Rehfield (1985), and Atilgan (1989), and Rehfield and Atilgan (1989), is 1.724 inch resulting in −7.6 percentage difference compared to the NASTRAN result.

The test data appearing in the comparisons of Figs. 4-9, are reported by Chandra *et al.* (1990), and Smith and Chopra (1990, 1991). Figures 4 and 5 show the bending slope variation along the beam span for antisymmetric and symmetric cantilevers under a 1 lb transverse tip load. The beam geometry and material properties are given in Table 5. The analytical predictions reported by Chandra *et al.* (1990), and Smith and Chopra (1990, 1991) together with results obtained on the basis of the

analyses of Rehfield (1985), Rehfield and Atilgan (1989), Atilgan (1989), and the present work are combined in Figs. 4 and 5. Results show that the predictions of the present theory are the closest to the test data when compared to the other analytical approaches.

The bending slope in Figs. 4 and 5 is defined in terms of the cross section rotation for theories including shear deformation. For the geometry and material properties considered, this effect is negligible as shown in Figs. 4 and 5 where the spanwise slope at the fixed end predicted by theories with shear deformation, is indistinguishable from zero. The nonzero value shown by the test data may be due to the experimental set up used to achieve clamped end conditions.

The spanwise twist distribution of symmetric cantilevered beam with $[30]_6$ and $[45]_6$ lay-ups is plotted in Figs. 6 and 7, respectively. The beams are subjected to a transverse tip load of 1 lb. Their dimensions and material properties are given in Table 5. Results show that the present theory and the works of Rehfield and Atilgan (1989) and Atilgan (1989) are the closest to the test data. A similar behavior is found for the bending slope and the twist angle at the mid-span of the symmetric cantilevered beams appearing in Figs. 8 and 9. The beams are subjected to a tip torque of 1 lb-in.

CONCLUSION

An anisotropic thin-walled closed section beam theory has been developed based on an asymptotical analysis of the shell energy functional. The displacement field is not assumed apriori and emerges as a result of the analysis. In addition to the classical out-of-plane torsional warping, two new contributions are identified namely, axial strain and bending warping. A comparison of the derived governing equations confirms the theory developed by Reissner and Tsai. In addition, explicit closed-form expressions for the beam stiffness coefficients, the stress and displacement fields are provided. The predictions of the present theory have been validated by comparison with finite element simulation, other closed form analyses and test data.

ACKNOWLEDGMENT

This work was supported by the NASA Langley Research Center under grant NAG-1-637. This support is gratefully acknowledged.

REFERENCES

Atilgan, Ali Rana, "Towards A Unified Analysis Methodology For Composite Rotor Blades," *Ph. D. Dissertation*, School of Aerospace Engineering, Georgia Institute of Technology, August 1989.

Armanios, Erian, Badir, Ashraf, and Berdichevsky, Victor, "Effect of Damage on Elastically Tailored Composite Laminates," *Proceedings of the AHS International Technical Specialists' Meeting on Rotorcraft Basic Research*, Georgia Institute of Technology, Atlanta, Georgia, March 25-27, 1991, pp. 48(1)-48(11).

Badir, Ashraf M., "Analysis of Advanced Thin-Walled Composite Structures," *Ph. D. Dissertation*, School of Aerospace Engineering, Georgia Institute of Technology, February 1992.

Berdichevsky, V. L., and Misiura, V., "Effect of Accuracy Loss in Classical Shell Theory," *Journal of Applied Mechanics*, December 1991.

Chandra, R., Stemple, A. D., and Chopra, I., "Thin-walled Composite Beams under Bending, Torsional, and Extensional Loads," *Journal of Aircraft*, Vol. 27, No. 7, July 1990, pp. 619-626.

Crandall, Stephen H., Dahl, Norman C., and Lardner, Thomas J., *An Introduction to the Mechanics of Solids*, McGraw-Hill Book Company, 1978.

Giavotto, V., Borri, M., Mantegazza, P., Ghiringhelli, G., Carmashi, V., Maffioli, G.C., and Mussi, F., "Anisotropic Beam Theory and Applications," *Computers and Structures*, Vol. 16, No. 1-4, pp. 403-413, 1983.

Gjelsvik, Atle, *The Theory of Thin Walled Bars*, John Wiley & Sons, 1981.

Hodges, D. H., "Review of Composite Rotor Blade Modeling," *AIAA Journal*, Vol. 28, No. 3, 1990, pp. 561-565.

Hodges, D. H., Atilgan A. R., Fulton M. V., and Rehfield L. W., "Dynamic Characteristics of Composite Beam Structures," *Proceedings of the AHS National Specialists' Meeting on Rotorcraft Dynamics*, Fort Worth, Texas, Nov. 13-14, 1989.

Jones, R. M., *Mechanics of Composite Materials*, McGraw Hill Book Co., New York, 1975, p. 163.

Koiter, W. T., "A Consistent First Approximation in the General Theory of Thin Elastic Shells," *Proc. IUTAM Symp on the Theory of Thin Shells*, Delft, August 1959, 12-33, North-Holland Publ. Amsterdam, 1960, Edited by W. T. Koiter.

Kosmatka, J. B., "Extension-Bend-Twist Coupling Behavior of Thin-Walled Advanced Composite Beams with Initial Twist," *Proceedings of the 32nd AIAA/ASME/-AHS/ASC Structures, Structural Dynamics and Materials Conference*, Baltimore, Maryland, April 8-10, 1991, pp. 1037-1049.

Libai, A., and Simmonds, J. G., *The Nonlinear Theory of Elastic Shells : One Spatial Dimension*, Academic Press, Inc., 1988.

Libove, C., "Stresses and Rate of Twist in Single-Cell Thin-Walled Beams with Anisotropic Walls," *AIAA Journal*, Vol. 26, No. 9, September 1988, pp. 1107-1118.

Mansfield, E. H., and Sobey, A. J., "The Fibre Composite Helicopter Blade - Part 1: Stiffness Properties - Part 2: Prospect for Aeroelastic Tailoring," *Aeronautical Quarterly*, Vol. 30,May 1979, pp. 413-449.

Megson, T. H. G., *Aircraft Structures for Engineering Students*, Second Edition, Halsted Press, 1990.

Nixon, M.W., "Analytical and Experimental Investigations of Extension-Twist-Coupled Structures," M.Sc. Thesis, George Washington University, May 1989.

Rehfield, L. W., "Design Analysis Methodology for Composite Rotor Blades," *Proceedings of the Seventh DoD/NASA Conference on Fibrous Composites in Structural Design*, AFWAL-TR-85-3094, June 1985, pp. (V(a)-1)-(V(a)-15).

Rehfield, L. W., and Atilgan, A. R., "Shear Center and Elastic Axis and Their Usefulness for Composite Thin-Walled Beams," *Proceeding of The American Society For Composites*, Fourth Technical Conference, Blacksburg, Virginia, October 3-5, 1989, pp. 179-188.

Rehfield, L. W., Atilgan, A. R., and Hodges, D. H.,"Nonclassical Behavior of Thin-Walled Composite Beams with Closed Cross Sections." *Journal of the American Helicopter Society*, Vol. 35, (2), April 1990, pp. 42-50.

Reissner E., and Tsai, W. T., "Pure Bending, Stretching, and Twisting of Anisotropic Cylindrical Shells," *Journal of Applied Mechanics*, Vol. 39, March 1972, pp. 148-154.

Sanders, J. L., "An Improved First-Approximation Theory for Thin Shells," *NASA - TR - R24*, 1959.

Smith, Edward C., and Chopra Inderjit, "Formulation and Evaluation of an Analytical Model for Composite Box-Beams," *Proceedings of the 31st AIAA/ASME/-AHS/ASC Structures, Structural Dynamics and Materials Conference*, Long Beach, California, April 2-4,1990, pp. 759-782.

Smith, Edward C., and Chopra Inderjit, "Formulation and Evaluation of an Analytical Model for Composite Box-Beams," *Journal of The American Helicopter Society*, July 1991, pp. 23-35.

Sokolnikoff, I. S., *Mathematical Theory of Elasticity*, McGraw-Hill, New York, 1956.

Timoshenko, S., and Goodier, J. N., *Theory of Elasticity*, McGraw-Hill, New York, 1951.

Vinson, J. R., and Sierakowski, R. L., *The Behavior of Structures Composed of Composite Materials*, Martinus Nijhoff Publishers, 1987., p.54.

Washizu, K., *Variational Methods in Elasticity and Plasticity*, Pergamon, New York, 1968.

Wempner, G., *Mechanics of Solids with Applications to Thin Bodies*, Sijthoff & Noordhoff International Publishers, 1981.

APPENDIX

In this appendix explicit expressions for some of the relevant variables used in the development as well as the stiffnesses C_{ij} $(i, j = 1, 4)$ in Eq. (42) are provided.

The three stiffness parameters A, B and C in Eq. (30) are expressed in terms of the Hookean tensor E^{ijkl} as follows

$$A(s) = < D^{1111} > - \frac{(< D^{1122} >)^2}{< D^{2222} >}$$

$$B(s) = 2\left(< D^{1112} > - \frac{< D^{1122} >< D^{1222} >}{< D^{2222} >} \right) \tag{53}$$

$$C(s) = 4\left(< D^{1212} > - \frac{(< D^{1222} >)^2}{< D^{2222} >}\right)$$

The $2D$ Young's moduli $D^{\alpha\beta\gamma\delta}$ are given by

$$D^{\alpha\beta\gamma\delta} = E^{\alpha\beta\gamma\delta} - \frac{E^{\alpha\beta 33}E^{\gamma\delta 33}}{E^{3333}} - H_{\mu\lambda}G^{\alpha\beta\mu}G^{\gamma\delta\lambda} \tag{54}$$

where

$$G^{\alpha\beta\mu} = E^{\alpha\beta\mu 3} - \frac{E^{\alpha\beta 33}E^{\mu 333}}{E^{3333}}$$

and $H_{\mu\lambda}$ are components of the inverse of the $2D$ matrix $\left\| E^{\mu 3\lambda 3} - \frac{E^{\mu 333}E^{\lambda 333}}{E^{3333}} \right\|$.

Combining Eq. (34) and (53) the variables b and c can be written as

$$b(s) = -\frac{< D^{1112} > - \frac{<D^{1122}><D^{1222}>}{<D^{2222}>}}{< D^{1212} > - \frac{(<D^{1222}>)^2}{<D^{2222}>}}$$

and

$$c(s) = \frac{1}{4\left(< D^{1212} > - \frac{(<D^{1222}>)^2}{<D^{2222}>}\right)} \tag{55}$$

where the pointed brackets denote integration over the thickness as defined in Eq. (9).

Expressions for the stiffness coefficients C_{ij} $(i, j = 1, 4)$ in terms of the cross section geometry and materials properties are as follows

$$C_{11} = \oint (A - \frac{B^2}{C})ds + \frac{[\oint (B/C)ds]^2}{\oint (1/C)ds}$$

$$C_{12} = \frac{\oint (B/C)ds}{\oint (1/C)ds} A_e$$

$$C_{13} = -\oint (A - \frac{B^2}{C})zds - \frac{\oint (B/C)ds \ \oint (B/C)zds}{\oint (1/C)ds}$$

$$C_{14} = -\oint (A - \frac{B^2}{C})yds - \frac{\oint (B/C)ds \ \oint (B/C)yds}{\oint (1/C)ds}$$

$$C_{22} = \frac{1}{\oint (1/C)ds} A_e^2 \tag{56}$$

$$C_{23} = -\frac{\oint (B/C)zds}{\oint (1/C)ds} A_e$$

$$C_{24} = -\frac{\oint (B/C)yds}{\oint (1/C)ds} A_e$$

$$C_{33} = \oint (A - \frac{B^2}{C})z^2 ds + \frac{[\oint (B/C)zds]^2}{\oint (1/C)ds}$$

$$C_{34} = \oint (A - \frac{B^2}{C})yzds + \frac{\oint (B/C)yds \ \oint (B/C)zds}{\oint (1/C)ds}$$

$$C_{44} = \oint (A - \frac{B^2}{C})y^2 ds + \frac{[\oint (B/C)yds]^2}{\oint (1/C)ds}$$

Figure Legends

Figure 1: Cartesian Coordinate System

Figure 2: Curvilinear Coordinate System

Figure 3: Beam Cross Section

Figure 4: Bending Slope of an Anti-Symmetric $[15]_6$ Cantilever Under 1 lb Transverse Tip Load

Figure 5: Bending Slope of a Symmetric $[30]_6$ Cantilever Under 1 lb Transverse Tip Load

Figure 6: Twist of a Symmetric $[30]_6$ Cantilever Under 1 lb Transverse Tip Load

Figure 7: Twist of a Symmetric $[45]_6$ Cantilever Under 1 lb Transverse Tip Load

Figure 8: Bending slope at mid-span under unit tip torque of Symmetric lay-up Cantilever beams

Figure 9: Twist at mid-span under unit tip torque of Symmetric lay-up Cantilever beams

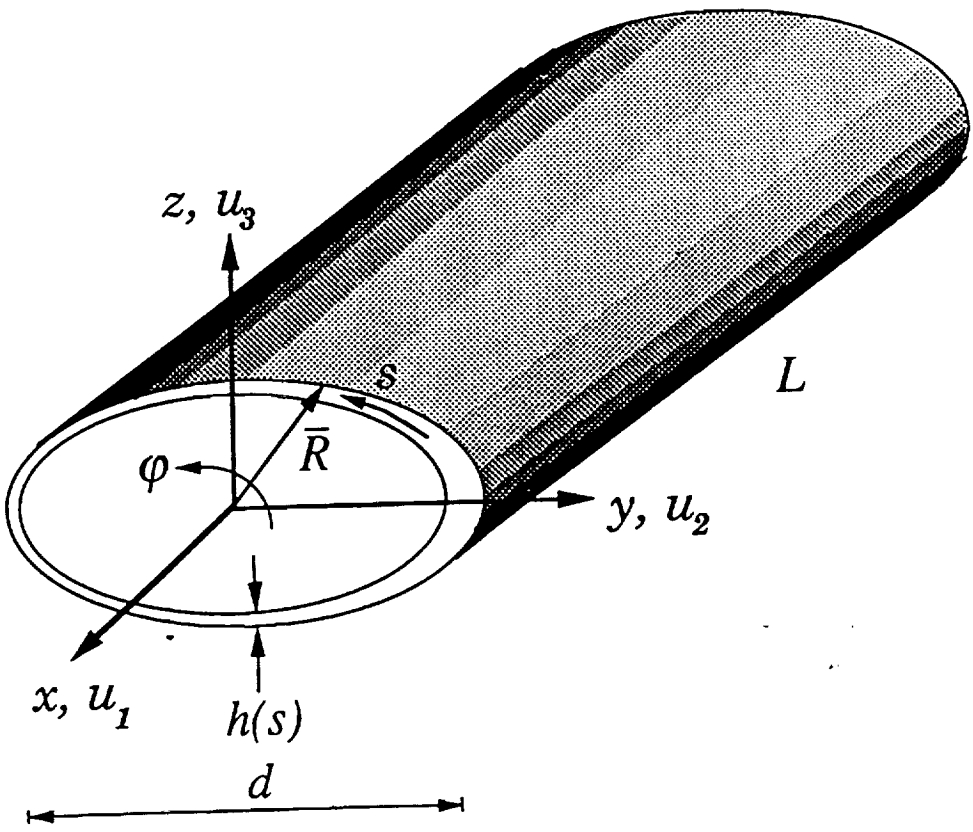
z, u3
s
L
φ
R̄
y, u2
x, u1
h(s)
d

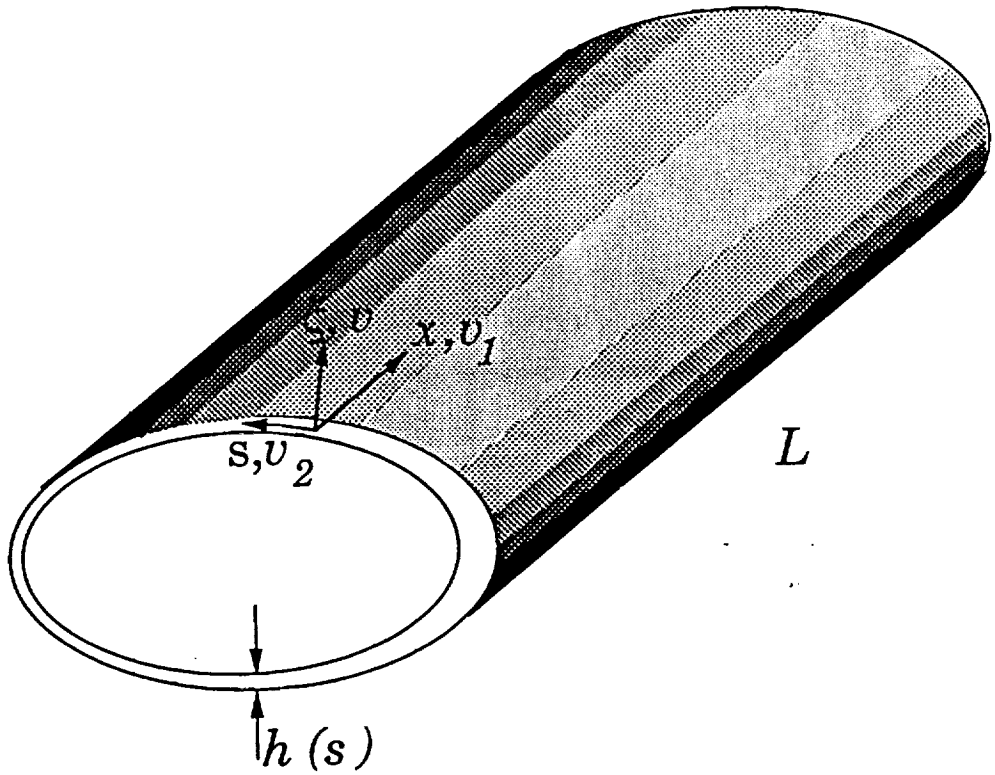
s, v
x, v1
s, v2
L
h (s)

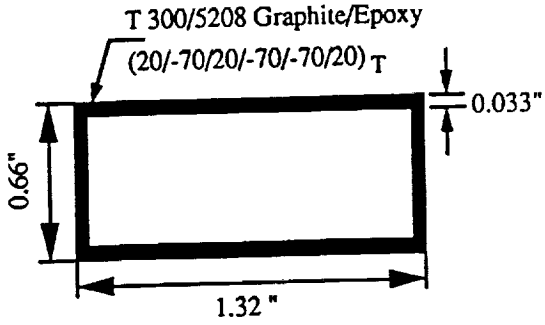
T 300/5208 Graphite/Epoxy
(20/-70/20/-70/-70/20) T
0.033"
0.66"
1.32 "

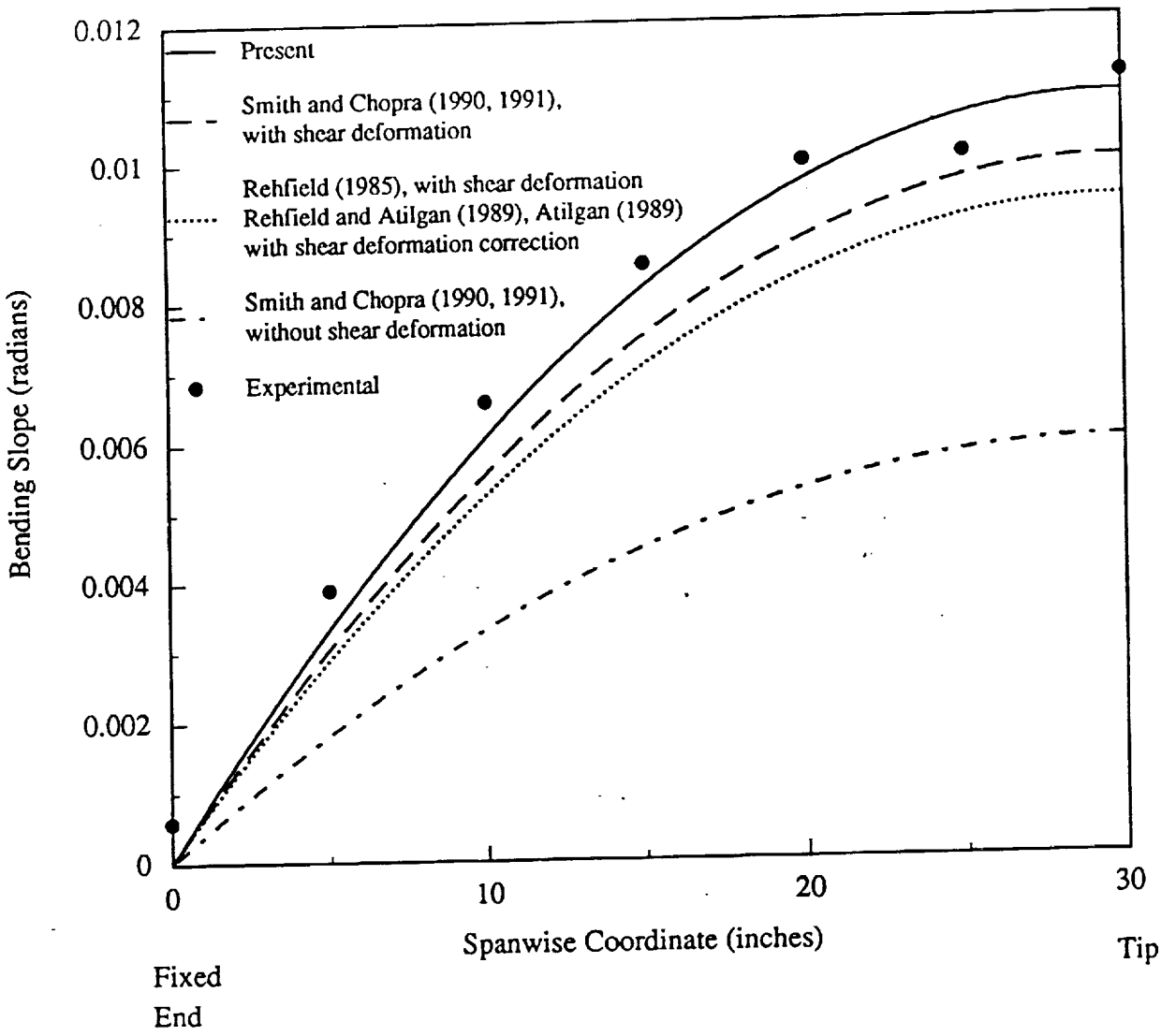
0.012
0.01
0.008
0.006
0.004
0.002
0
Bending Slope (radians)
Present
Smith and Chopra (1990, 1991), with shear deformation
Rehfield (1985), with shear deformation
Rehfield and Atilgan (1989), Atilgan (1989) with shear deformation correction
Smith and Chopra (1990, 1991), without shear deformation
Experimental
0
10
20
30
Spanwise Coordinate (inches)
Fixed End
Tip

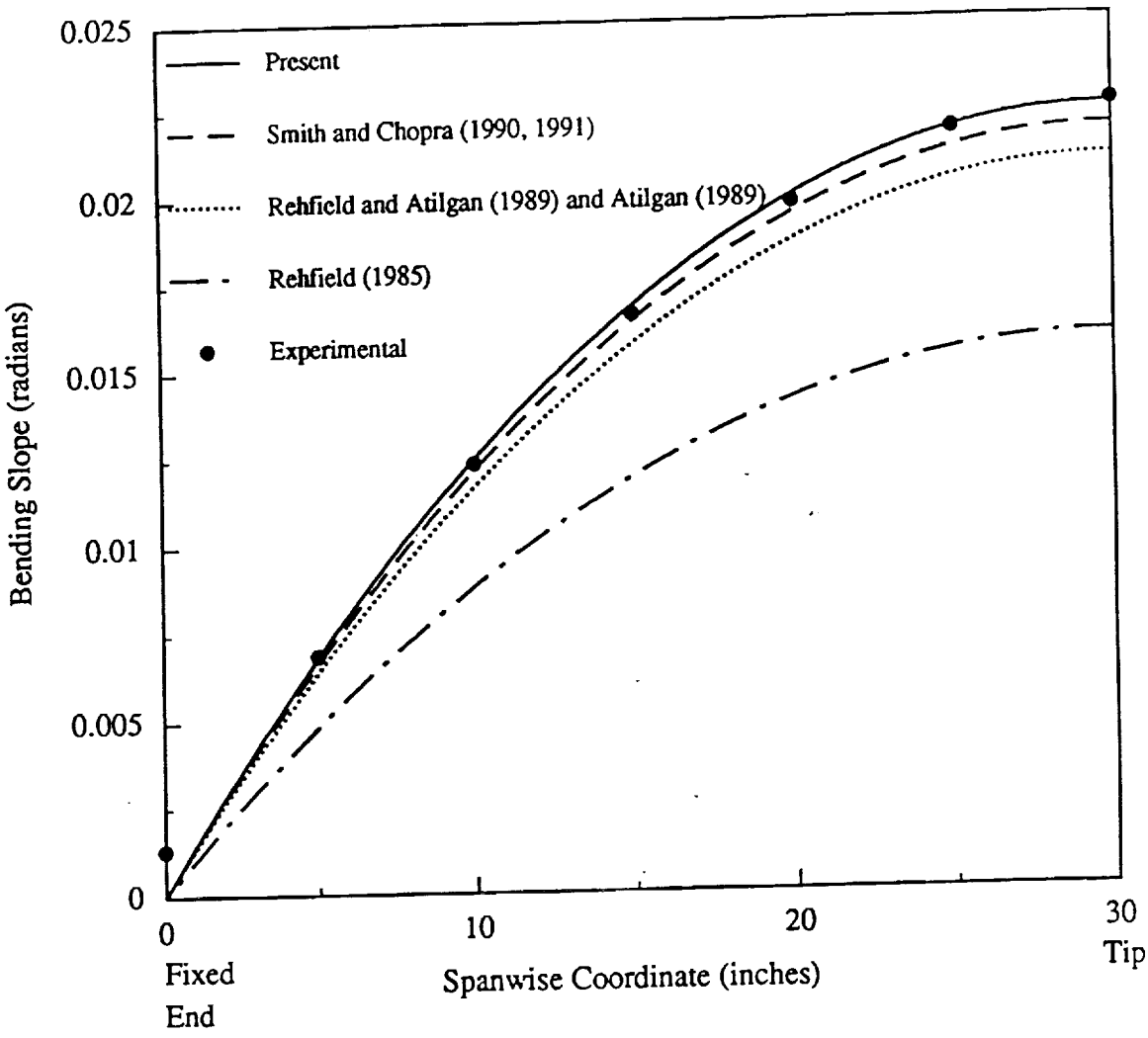
0.025
0.02
0.015
0.01
0.005
0
Bending Slope (radians)
Present
Smith and Chopra (1990, 1991)
Rehfield and Atilgan (1989) and Atilgan (1989)
Rehfield (1985)
Experimental
0
Fixed End
10
20
30
Tip
Spanwise Coordinate (inches)

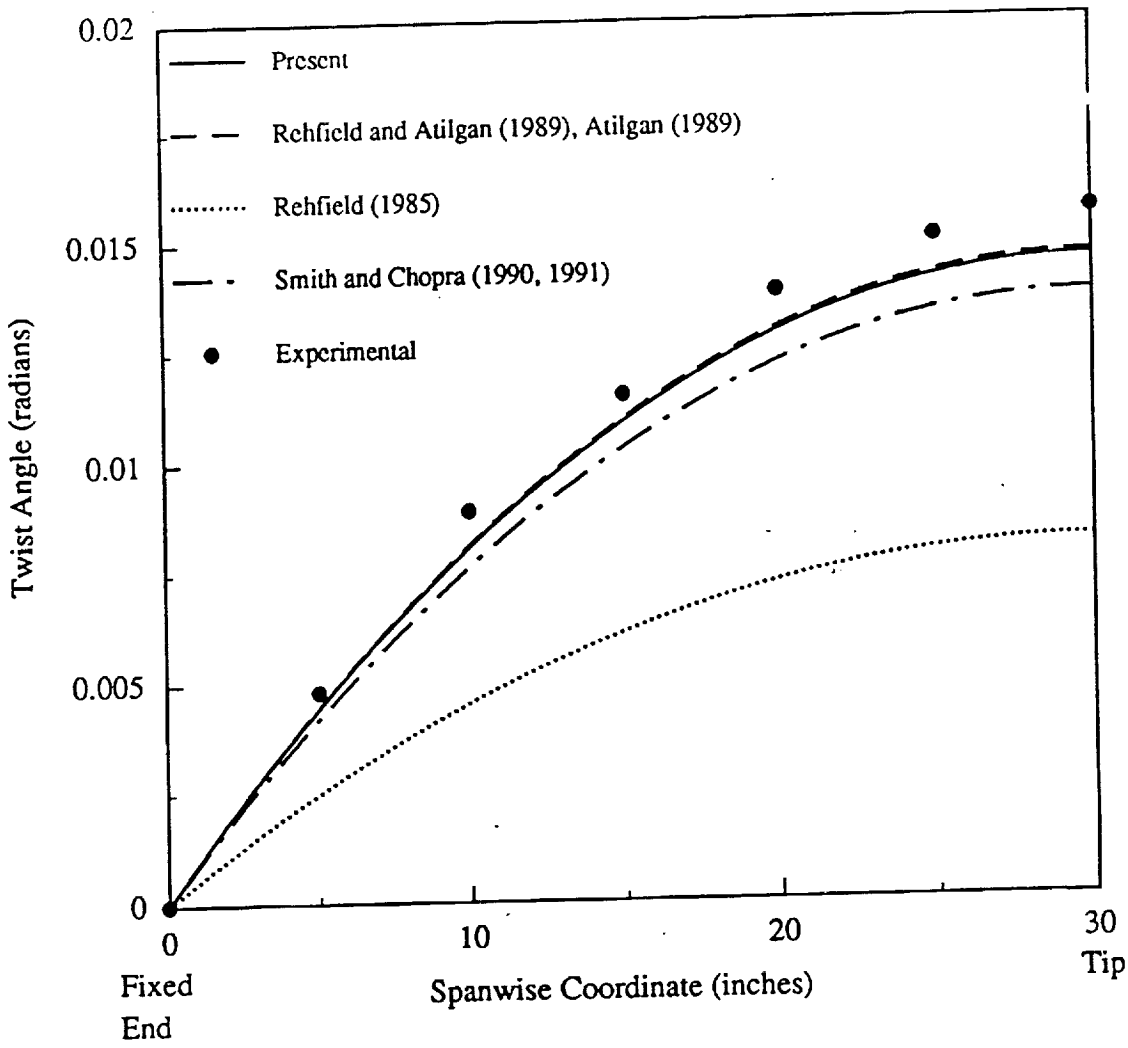
0.02
0.015
0.01
0.005
0
Twist Angle (radians)
Present
Rehfield and Atilgan (1989), Atilgan (1989)
Rehfield (1985)
Smith and Chopra (1990, 1991)
Experimental
0
Fixed End
10
20
30
Tip
Spanwise Coordinate (inches)

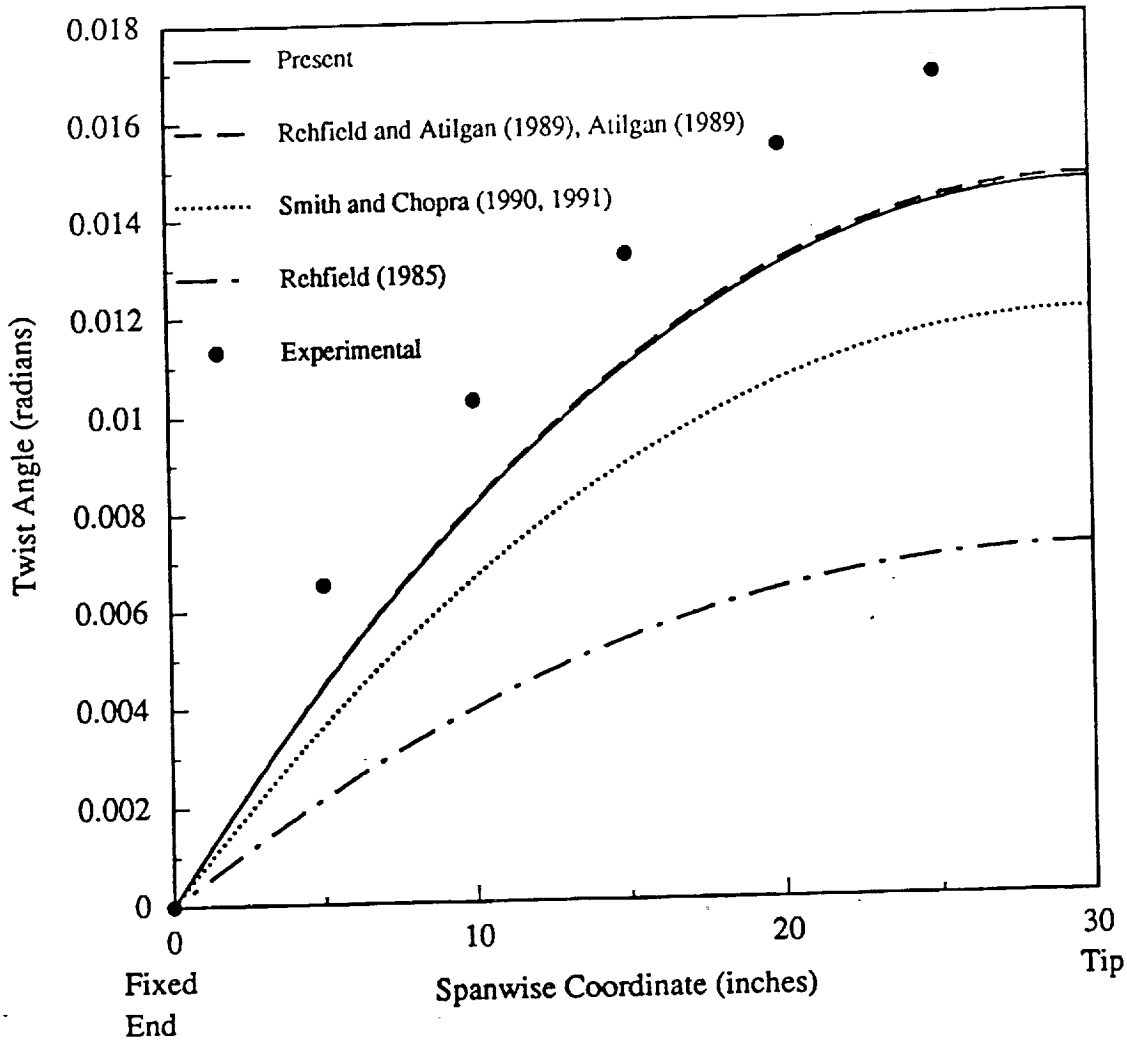
0.018
0.016
0.014
0.012
0.01
0.008
0.006
0.004
0.002
0
Twist Angle (radians)
Present
Rehfield and Atilgan (1989), Atilgan (1989)
Smith and Chopra (1990, 1991)
Rehfield (1985)
Experimental
0
Fixed End
10
20
30
Tip
Spanwise Coordinate (inches)

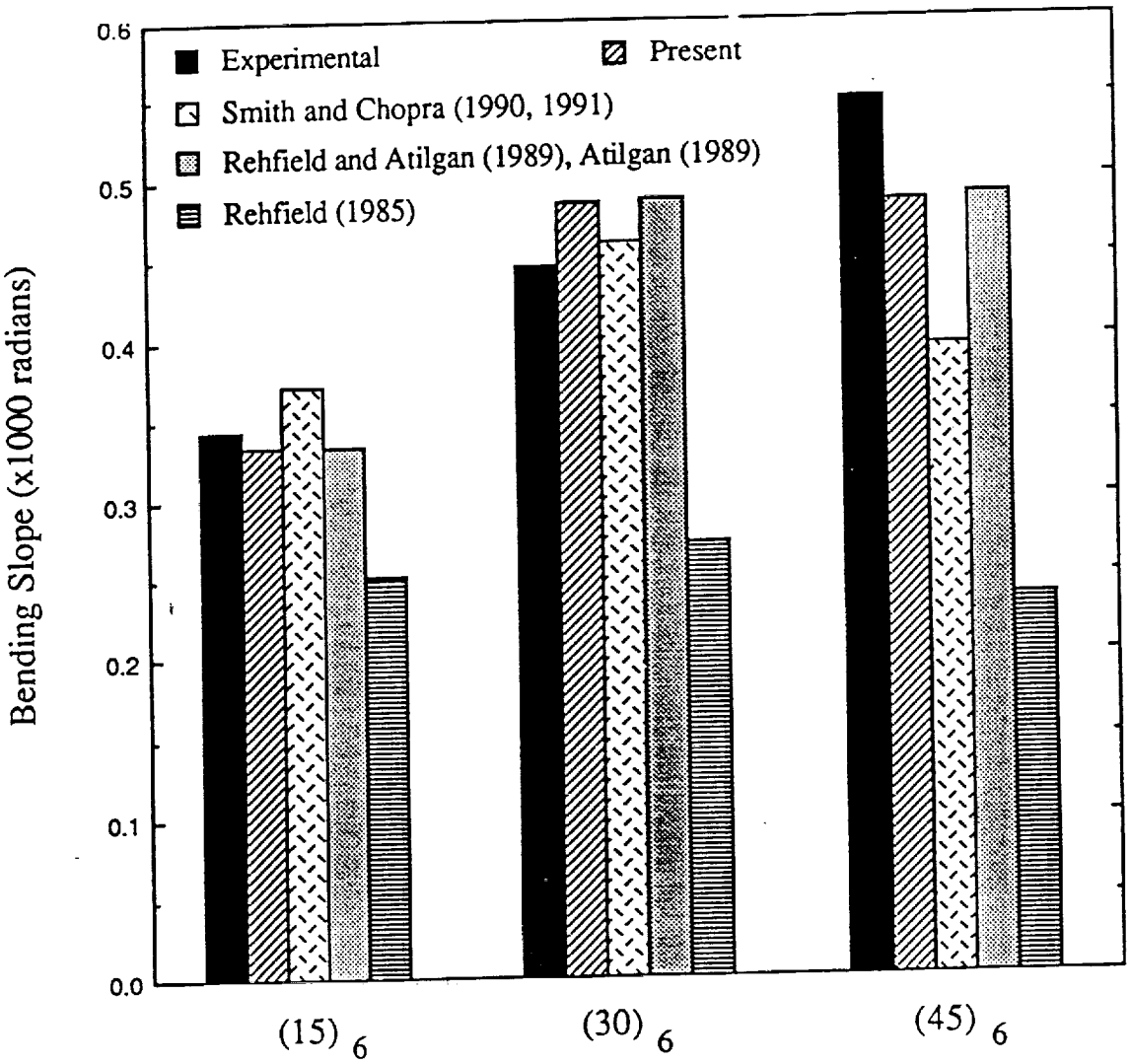
Experimental
Present
Smith and Chopra (1990, 1991)
Rehfield and Atilgan (1989), Atilgan (1989)
Rehfield (1985)
Bending Slope (x1000 radians)
0.0
0.1
0.2
0.3
0.4
0.5
0.6
(15) 6
(30) 6
(45) 6

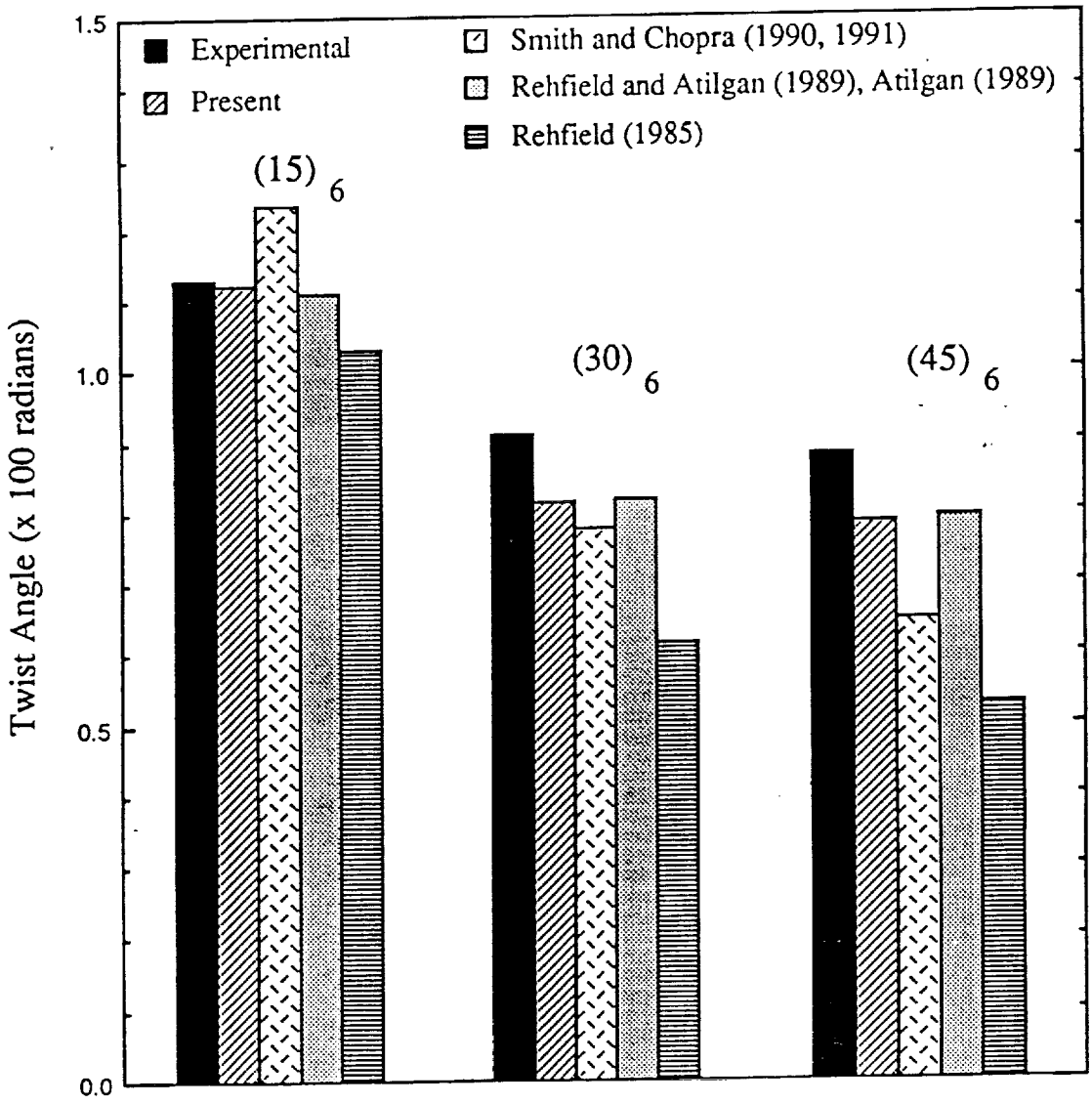
Experimental
Present
Smith and Chopra (1990, 1991)
Rehfield and Atilgan (1989), Atilgan (1989)
Rehfield (1985)
(15) 6
(30) 6
(45) 6
Twist Angle (x 100 radians)
1.5
1.0
0.5
0.0